Effect of environmental enrichment on airflow based learning

A Thesis

submitted to

Indian Institute of Science Education and Research Pune in partial fulfilment of the requirements for the BS-MS Dual Degree Programme
by

Meher Kantroo
20151107

Indian Institute of Science Education and Research Pune
Dr. Homi Bhabha Road,
Pashan, Pune 411008, INDIA.

29th March, 2020

Supervisor: **Dr. Nixon M. Abraham**

At the

Department of Biology
Indian Institute of Science Education and Research Pune

Certificate

This is to certify that this dissertation entitled "**Effect of environmental enrichment on airflow based learning**" towards the partial fulfilment of the BS-MS dual degree programme at the Indian Institute of Science Education and Research, Pune represents study/work carried out by Meher Kantroo at Indian Institute of Science Education and Research under the supervision of Dr. Nixon M. Abraham, Assistant Professor, Department of Biology, during the academic year 2019-2020.

Meher Kantroo

Dr. Nixon Abraham

Declaration

I hereby declare that the matter embodied in the report entitled entitled "**Effect of environmental enrichment on airflow based learning**" are the results of the work carried out by me at the Department of Biology, Indian Institute of Science Education and Research, Pune, under the supervision of Dr. Nixon M. Abraham and the same has not been submitted elsewhere for any other degree

Meher Kantroo

Dr. Nixon Abraham

Contents

Abstract

A non-canonical yet imperative function of the rodent olfactory system is to process airflow related information. Studies from our laboratory, involving surgical and optogenetic modification of the Olfactory Bulb (OB) circuitry has determined its role in airflow detection and discrimination. This was further confirmed in transgenic mice in which a subunit of glutamatergic AMPA receptors (GluA2) was knocked down heterozygously from GAD2 expressing interneurons (GAD2GluA2$^{\Delta ht}$ mice). These mice were unable to accurately discriminate between two airflows. While it is known that Environmental Enrichment (EE) can lead to better learning and memory, we aimed to test its efficacy in observed sensory deficit in GAD2GluA2$^{\Delta ht}$ mice. Our EE paradigm also included olfactory and somatosensory enrichment. To test the effect of EE, we carried out Go/No-Go odor and flow discrimination training while animals were living in the enriched environment. EE resulted in the rescue of learning deficits observed in airflow information processing abilities of GAD2GluA2$^{\Delta ht}$ mice. In addition, EE led to faster learning pace in a flow coupled with odor discrimination task. As a first step in probing the neural mechanisms underlying the rescue of learning deficits in enriched GAD2GluA2$^{\Delta ht}$ mice, we investigated changes in neural activity marker c-Fos and adult neurogenesis (using BrdU) in OB. Immunohistochemistry and imaging using confocal microscopy was performed in order to quantify c-Fos activation and BrdU positive cells in OB. As compared to the non-enriched group, there was increased OB interneuronal activation observed in enriched group. However, there was no EE dependent increase in OB adult neurogenesis. Our findings call for further experiments dissecting physiological changes in OB circuitry of EE and non-EE mice, which will help us establishing the causality of observed behavior.

List of figures

List of tables

Acknowledgements

I would like to express my gratitude to my supervisor, Dr. Nixon M. Abraham for his mentorship and continuous guidance throughout my thesis work. His valuable suggestions and important inputs immensely helped me during my project. I am also grateful to my TAC member, Dr. Raghav Rajan for his insightful suggestions and encouragement.

I would also like to especially thank my mentor Meenakshi Pardasani who not only taught me the necessary techniques, but also guided and encouraged me throughout the project. I am grateful to Shruti, Sarang and Anindya for their guidance and stimulating discussions. I would also like to acknowledge and thank all other lab members of Laboratory of Neural Circuits and Behavior (LNCB) for making me feel at home: Atharva, Felix, Rajdip, Priya, Arpan, Sanyukta, Avi, Kishalay, Lisni, Rishabh and Shivangi.

I am grateful to NFGFHD, IISER Pune for timely providing animals for my thesis work. I would also like to thank the Microscopy facility of IISER Pune for allowing me to make use of confocal microscopy facility.

Finally, I am extremely thankful to my family-parents, sister, aunt and grandmothers who continued to support and motivate me throughout the year. I wish to thank my friends, for all the light hearted discussions, motivation and fond memories that they have given me.

1. Introduction

Our sensory organs collect information from a constantly changing environment in order to feed, reproduce, escape predators or hunt preys. Information pertaining to different kinds of stimuli is gathered by different sensory systems and processed by the respective brain regions. It is also possible for a particular sensory system to process more than one kind of stimuli. Olfactory system is responsible for collecting and perceiving odor related information. Other than odor information, the olfactory system can sense mechanical as well as thermal information (Minghong Ma, 2009).

At the anatomical level, olfactory system consists of Nasal Cavity, a pre-cortical processing area called the Olfactory Bulb (OB) and Olfactory Cortex (OC). The Nasal Cavity contains the Main Olfactory Epithelium (MOE). The olfactory system also contains several sub-systems. The Gruenberg Ganglion (GG), responds to cold temperature and alarm signals (Bumbalo et al., 2017). The Septal Organ (SO) responds to stimuli which are mechanical in nature (Grosmaitre et al., 2007). Vomeronasal Organ (VNO) is involved in pheromonal signaling.

The odor molecules reach the nasal cavity in the form of plumes which is also associated with different airflows. It is not known how the turbulent nature of odor plumes and aerodynamics within the turbinates of the nasal cavity can affect the odor perception (Zhao and Frye, 2015). Moreover, there are varying levels of odor concentrations and gradients in the environment. It is possible that due to the changing spatiotemporal dynamics of odor concentration, the olfactory system might use mechanical cues in order to form a better odor percept.

All odor information is first collected by the MOE, which comprises of Olfactory Sensory Neurons (OSNs). The stimulus information from here is then carried to OB, the first relay station for olfactory information processing. The final stage of processing occurs in the higher-order cortical areas. OB has been shown to be responsive to odorless Ringer's puffs (Ueki et al., 1961). Studies have also established that OSNs, in particular, are also responsive to the Ringer's puffs (Grosmaitre et al. 2007). However, these studies have been performed in an *in vitro*

preparation. Despite, *In vivo* studies probing the mechanical information processing that could be brought about by airflows associated with odor plumes remains unclear.

Often, the whisker system has been studied in relation to airflow information processing. Being nocturnal animals, mice use their whiskers to localize objects and differentiate between different textures (Arabzadeh et al., 2003). Whiskers help the animals to navigate in the dark by aiding in discrimination between objects having different tactile properties (for example, a rough or a smooth textured surface). As a whisker interacts with its surrounding environment, it moves in a to and fro manner. This information in the form of physical deflection is carried to the mechanoreceptors located at the base of whisker follicles (Boubenec et al., 2012). The mechanoreceptors are responsible for the conversion of mechanical information into electrical signals. Finally, the neural signals (electrical information) are carried to higher-order cortical areas via the trigeminal nucleus and thalamus (Arabzadeh et al., 2004). In cortical area, the representation of each whisker is in the form of a barrel, thus, named as barrel cortex (Woolsey & Van der Loos, 1970).

A recent study investigated the role of whiskers in an airflow localization task. Airflow, being a mechanical stimulus, activates the whisker mechanoreceptors and lead to further sensory processing (Yu et al., 2016). In this study, rats underwent behavioral training where they were exposed to a circular area containing five holes located around the circumference. Fans creating airflow were present in each of these five holes. For one particular trial, one of the holes would expel the air. The accuracy with which the rats would follow the airflow to receive a reward (food) was investigated. While rats performed this associative task accurately in the presence of whiskers, upon whisker removal, a drop in the accuracy was observed (Yu et al., 2016). This highlighted a role of the whisker system in airflow information processing. Even though the accuracy decreased, it was still significantly above chance level. If the whisker system was wholly responsible for airflow processing, the accuracy would have dropped down to the chance level. However, this was not observed. Thus, it can be predicted that apart from the whisker system, some other sensory system is also involved in processing of airflow information. As the OSNs are responsive towards mechanical stimuli, it is possible that it is involved in airflow

information processing. Unpublished data from our lab points to the fact that the olfactory system is indeed involved in airflow information processing. Mice are able to discriminate between two different airflow rates. The OB was surgically removed from experimental mice, following which, mice showed chance level performance in airflow discrimination tasks. Also, in another set of experiments, the OSNs were washed off by zinc sulphate. As a result, mice were unable to discriminate between different airflow rates. Thus, OB has been shown to be pertinent to airflow information processing (Sarang Mahajan, LNCB, Unpublished Data).

1.1. Processing of Olfactory Information

Odor molecules are carried by wind to the nasal cavity of animal. The nasal cavity contains a sheet of epithelial tissue called the MOE which contains the sensory neurons (Nagayama et al., 2014). These OSNs contain numerous types of Olfactory Receptors (ORs). Embedded in the cilia of sensory neurons, ORs are a type of seven transmembrane G-protein coupled Receptors (GPCRs). Incoming volatile odor molecules bind to the ORs and activate a downstream secondary messenger pathway (Getchell et al., 1984). The binding of an odor molecule to a receptor leads to activation of G_{olf}, a GPCR. Further, G_{olf} binds to guanosine triphosphate (GTP) and activates the enzyme called Adenylyl Cyclase III (ACIII). This enzyme is responsible for the production of cyclic adenosine monophosphate (cAMP). The role of cAMP is to bind to cyclic nucleotide gated (CNG) channels. Finally, this binding results in the opening of CNG channels and an influx of calcium (Ca^{2+}) and sodium (Na^{+}) ions. The influx of ions leads to the generation of an action potential (AP) which travels via the sensory neurons and reaches the OB for further processing (Imai & Sanako, 2008).

The axon terminals of OSNs which travel to the OB, form synapses with the projection neurons in neuropil-like structures called glomeruli (Figure 1). A single OSN expresses one type of OR. All sensory neurons expressing the same type of the OR converge onto the same glomerulus. Mitral/Tufted (M/T) cells, which are the projection neurons of the OB, send information to higher-order cortical areas such as Anterior Olfactory Nucleus (AON), Piriform Cortex (PC), etc. (Mori & Sakano, 2011).

One of the major players of the OB neural circuitry is the population of local interneurons. There are majorly two types of interneurons present in the bulb: Periglomerular cells (PGCs) and Granule Cells (GCs). Most of these cells are inhibitory and release the neurotransmitter gamma-aminobutyric acid (GABA) onto the M/T cell population (Shepherd et al., 2004). PGCs are located in the Glomerular Layer (GL) and get directly (as well as indirectly) excited by the OSNs. Granule cells are embedded within the Granule Cell Layer (GCL). GCs are also present in the Mitral Cell Layer (MCL). GCs modulate the OB activity via lateral and recurrent inhibition. When a granule cell is excited by a M/T cell, it can inhibit either the same M/T cell (recurrent inhibition) or a different M/T cell (lateral inhibition) (Shepherd et al., 2007).

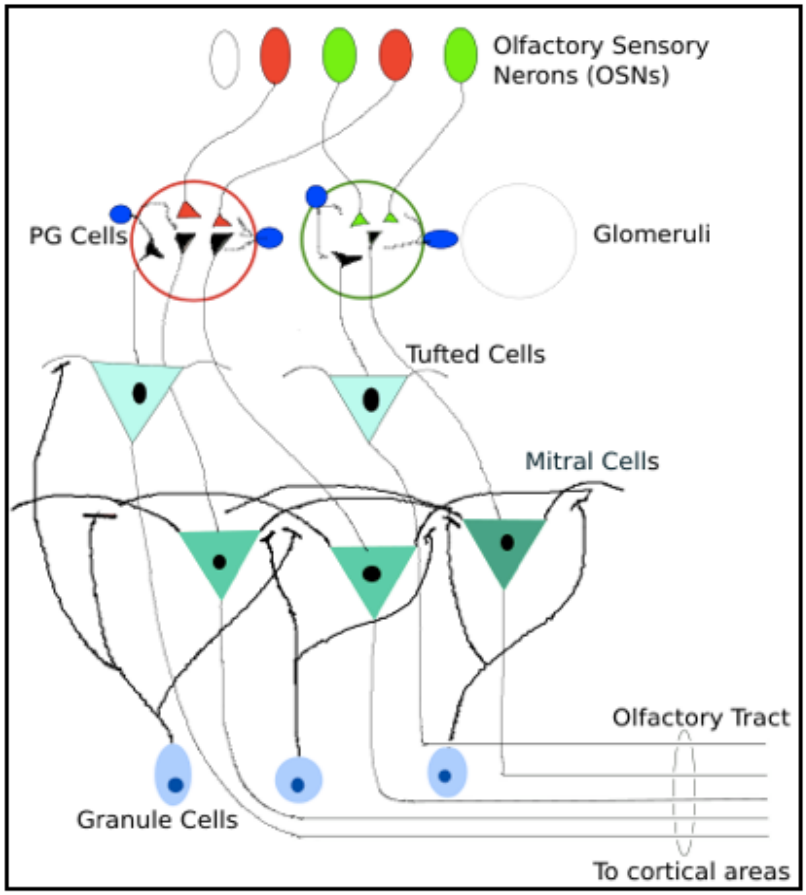

Figure 1. Organization of the neural circuit in Olfactory Bulb. OSNs line the Olfactory Epithelium. Axon terminals of OSNs travel to OB and converge into glomeruli at the GL. Red colored OSNs express a particular type of receptor while green colored OSNs express another type of receptor. As shown, OSNs expressing a particular type of receptor converge to the same glomerulus. Synapses are formed between OSNs and M/T cells at the GL. Next layer contains some interneurons and dendrites of the M/T cells in the External Plexiform Layer (EPL). MCL contains cell bodies of

M/T cells. Granule cells present in GCL start their branching just outside the M/T cell body layer. *Finally, the M/T cell axons project to cortical areas via the olfactory tract.*

A significant functional role of the local inhibitory interneurons is to control the spiking rate of M/T cells and increase the signal to noise ratio of the output going to the olfactory cortex (Isaacson & Strowbridge, 1998). Lateral inhibition, in particular, helps increase the contrast between odor representations by inhibiting the nearby M/T cells (Margrie et al., 2001). The projection neurons of the OB also have a characteristic synchronous activity. Upon odor exposure, oscillations in the gamma range (between 30 and 80Hz) have been recorded in the M/T cells (Rall & Shepherd et al., 1968). The inhibitory activity of the GCs modulates the synchrony of the oscillations. Blocking the inhibitory interneuronal activity showed a drastic decrease in the synchronous gamma oscillations, which ultimately led to the formation of an altered olfactory map (Lagier et al.,2004). The other interesting aspect of the OB interneurons is their ability to undergo adult neurogenesis (formation of neurons during adulthood) (Lledo et al., 2006). Neuroblasts are formed in the sub-ventricular zone (SVZ) and migrate to the OB via the rostral migratory stream (RMS). The generation and survival of adult born interneurons is also highly activity dependent. An increase in the survival rate of GCs was observed after olfactory enrichment (Rochefort et al., 2002). A marked decrease in the number of adult born GCs was observed due to olfactory deprivation by nostril occlusion (Yamaguchi & Mori, 2005). Thus, the OB interneurons are chiefly important for the proper functioning of the OB neural circuitry. Modulation in the activity and generation of OB interneurons could further advance out knowledge of their role in airflow information processing.

The OB interneurons are activated when OSNs and M/T cells release Glutamate onto the ionotropic glutamate receptors of PGCs and GCs. These activated interneurons, in turn, release GABA onto the ionic GABAergic receptors of M/T cells. There are three types of ionotropic Glutamate receptors (iGluRs): alpha-amino-3-hydroxy-5-methyl- 4-isoxazolepropionic acid (AMPA), N-Methyl-D-Aspartic acid (NMDA) and kainate receptors.

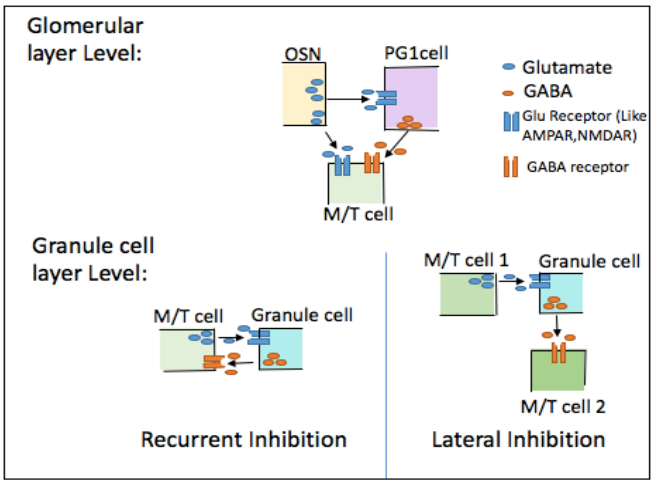

Figure 2. Interactions between OB interneurons, OSNs and M/T cells. At the level of GL, OSNs release Glutamate onto the glutamate receptors (AMPA and NMDA) of PG cells, thus activating them. PG cells release GABA that binds to GABA receptors of M/T cells. At the GCL, M/T cells release glutamate onto AMPA or NMDA receptors of GCs. These GCs in turn release GABA which binds to GABA receptors of either the same or a different M/T cell.

Both glutamate and GABA receptors play a vital role in the functioning of the interneurons. At the GL, OSNs release glutamate onto both M/T cells and PG cells. This leads to activation of the iGluRs (AMPARs, NMDARs and kainate receptors) of the PGCs as well as M/T cells. Due to the binding of glutamate to its receptors on PGCs cells, downstream signaling occurs which leads to release of GABA from PG onto the M/T cell. At the GCL, excited M/T cells release Glutamate onto the NMDA or AMPA receptors of the granule cells. The inhibitory granule cells, thus, release GABA onto the GABA receptors of the same (recurrent inhibition) or neighboring (lateral inhibition) M/T cell (Figure 2).

AMPA receptor contains four subunits: GluA1, GluA2, GluA3 and GluA4 (Sobolevsky et al., 2009). Calcium permeability of AMPA receptor depends on the GluA2 subunit. In GluA2, a post-transcriptional modification takes place wherein a codon encoding Glutamine (Gln, Q) is modified into a codon encoding Arginine (Arg, R). This is called Q/R RNA editing (Wright & Vissel, 2012). If Q/R editing does not take place, the AMPA receptor is calcium-permeable. Also, if the AMPA receptor is lacking the GluA2 subunit, the receptor is permeable to calcium (Burnashev et al., 1996). In recent years, studies have provided evidence for a link between calcium-permeable

AMPA receptors (CP-AMPARs) and disorders such as Amyotrophic Lateral Sclerosis (ALS) (Kwak & Kawahara, 2005). GluA2 is also responsible for the regulation of AMPA receptor trafficking at the synapse. One approach to study airflow information processing by OB is to modulate the action of the receptors present on the neurons involved in this process. In our lab, we have access to heterozygous GluA2 knockout mice lines (Courtesy: Rolf Sprengel), which have been created using the Cre-lox system. The GluA2 subunit had been knocked out partially from the interneuronal population which express the glutamate decarboxylase (GAD2) enzyme (GAD2GluA2$^{\Delta ht}$). GABA is synthesized by either GAD1 or GAD2 enzyme (Wu et al., 2007). Around 59% of OB neurons express GAD2 enzyme whereas around 51% express GAD1 enzyme. Also, 80% of neurons co-express GAD1 and GAD2 (Parrish et al., 2007). In a study published in 2010, GluA2 subunit was knocked out selectively from the GCs of OB. A faster discrimination time for complex odor mixtures was observed in this case (Abraham et al., 2010). Airflow discrimination abilities have been checked in GAD2GluA2$^{\Delta ht}$ to investigate the role of inhibitory interneurons in airflow discrimination tasks. It has been observed that the GAD2GluA2$^{\Delta ht}$ have deficits in airflow discrimination, i.e., they were unable to accurately discriminate between different airflow rates.

1.2. Environmental Enrichment as a therapeutic intervention

Is it possible to improve the observed airflow deficit in the GAD2GluA2$^{\Delta ht}$ by using an Environmental Enrichment (EE) paradigm? Compared to standard laboratory animal housing, an EE paradigm refers to a housing condition with increased space, greater number of house mates as well as additional toys for cognitive stimulation such as mazes, tunnels and running wheels (Rosenzweig et al., 1996). Donald O Hebb, famous for his work on synaptic plasticity, was one of the first few researchers to investigate the enriching effects of an environment. He observed that rats exposed to an enriched environment had enhanced cognitive skills as compared to laboratory bred mice. Hebb's enriched mice performed better at solving mazes as compared to the non-enriched ones (Brown & Milner, 2003). Since then, numerous studies have investigated the remarkable effects of EE paradigm in conditions ranging from stroke and trauma to visual deficits. In animal models of Retinitis Pigmentosa (RP), there is

decline in the number of rods and cones photoreceptors, leading to gradual loss of vision. Exposing RP animal models to EE has shown to slow down the vision loss. There is a delay in the degeneration of rods and cones. As opposed to non-enriched RP models, the enriched ones had a higher visual acuity and performed better in visual behavioural tasks (Barone et al., 2014). In another study, EE was shown to cause increase in neuronal responses in the auditory cortex of rats. There was improvement in selectivity as well as sensitivity of the cortical neuron responses (Engineer et al., 2004).

Several factors have been implicated as the possible causes of EE benefits. These can be broadly divided into anatomical changes to neurons (and the brain) as well as biochemical changes in the brain environment. At the structural level, the size as well as weight of the brain increases on EE exposure (Bennett et al., 1969). After EE exposure, neurons of the animals have a greater number of synapses and an increased dendritogenesis (Jung & Herms, 2014). Numerous studies have also shown an increased level of hippocampal adult neurogenesis due to an EE paradigm (Kempermann et al., 1997). At a molecular stage, increase in various neurotropic as neurotransmitter levels has been observed. In particular, increase in Brain Derived Neurotrophic Factor (BDNF), which has been connected to better learning as well as increased neurogenesis, has been seen (Pham et al.,1999). Levels of neurotransmitter such as serotonin and acetylcholine also increase in an EE paradigm (Koh et al., 2007; Por et al., 1982). These, among various other factors collectively act together to benefit an animal exposed to an enriched environment (Figure 3).

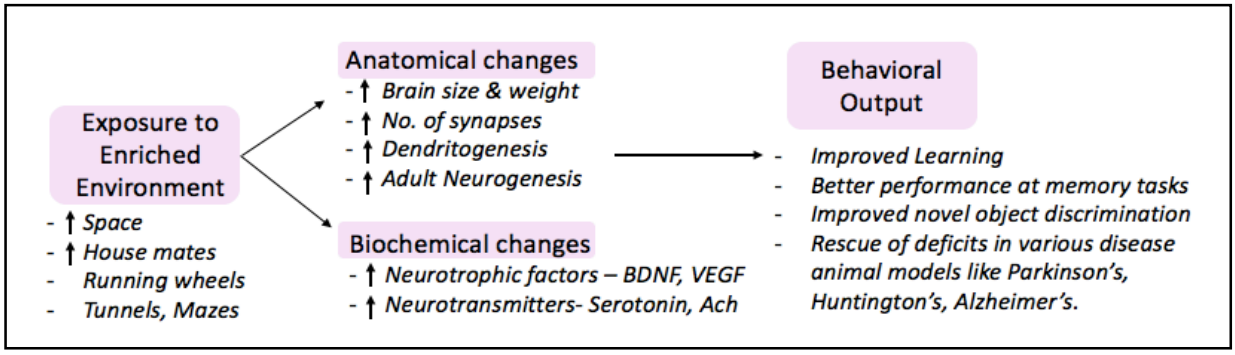

Figure 3. Summary of the benefits of Environmental Enrichment paradigm (Adapted from Alwis & Rajan, 2014; Kempermann, 2019)

In our environmental enrichment paradigm, there is social, motor, tactile and cognitive stimulation. Since OB is playing a role in airflow processing, an interesting question to ask is whether olfactory enrichment could also lead to an improvement in the deficit in case of GAD2GluA2$^{\Delta ht}$. Olfactory enrichment has been shown to improve odor discrimination abilities. It also influences adult neurogenesis in the OB (Bonzanno et al., 2014). Unpublished data from our lab suggests that in animal models of Early Life Stress (ELS), exposure to an enriched environment including olfactory enrichment using natural odors, leads to improvement in odor discrimination abilities. Environmentally enriched ELS mice also show an increase in OB adult neurogenesis (Meenakshi Pardasani, LNCB, Unpublished Data). Apart from this, there is also somatosensory stimulation in our paradigm, which would stimulate the whisker system. Enrichment has shown to also affect the whisker map in the S1 area of cortex. In wild type mice, the layer 2/3 (L2/3) of the S1 cortical area shows a salt and pepper representation of neurons with poorly defined functional boundary. Enrichment led to sharpening of L2/3 neurons and formation of a functional boundary between L2 and L3. This would lead to improved neural coding of the whiskers in the cortical area and improvement in touch detection by the animals. (Lemessurier et al., 2019).

The objective of this thesis is to investigate whether an enriched environment could be used as a therapeutic intervention in case of the airflow discrimination learning deficit observed in GAD2GluA2$^{\Delta h}$ mice. The effect that EE exposure would have on airflow based learning remains elusive. It is not known whether transgenic mice with a sensory deficit in airflow discrimination abilities would show an improvement when exposed to EE. The hypothesis is that EE (including olfactory and somatosensory enrichment) would lead to a rescue in the observed sensory deficit in GAD2GluA2$^{\Delta h}$ mice. Thus, this thesis will focus on the dynamics between nature (lack of GluA2 subunit leading to sensory deficit) and nurture (possible rescue due to EE).

As a part of my thesis project, I have investigated the effects of environmental enrichment paradigm on the airflow and odor discrimination abilities of GAD2GluA2$^{\Delta h}$ mice. EE paradigm has been used to check whether enrichment, including the olfactory and somatosensory kind, can rescue the deficits observed in

airflow discrimination. As compared to non-enriched GAD2GluA2$^{\Delta h}$ mice, the enriched mice were significantly better at airflow discrimination tasks. Thus, EE exposure showed improvement in airflow deficits observed in GAD2GluA2$^{\Delta h}$ mice. Furthermore, immunohistochemistry has been performed to investigate the neural correlate of the observed improvements.

2. Materials & Methods

2.1. Animals

The following group of mice were used for all the experiments performed within the scope of this thesis:

Sr. No.	Animal Strain	Age	No. of animals
1.	C57BL6J Wild-type	6-8 weeks	12
2.	GAD2GluA2$^{\Delta ht}$ (ht-heterozygous)	6-8 weeks	21

Table 1. Strain of the animals, age and number of animals used.

We had access to GluA2-Gad2 mice lines which were created using the Cre-Lox approach. Gria2^{2lox} mice were crossed with Gad2 cre mice. In Gria2^{2lox} mice, GriA2, the gene which undergoes transcription and translation to form GluA2 as the product, is flanked by two lox sites. In GAD2 cre mice, the cre sites are under the GAD2 promoter of all interneurons. In the F1 generation, cre enzyme recombined with the loxP sites carrying target gene GluA2 leading to excision of GluA2 from cell populations expressing Gad2. The mice were kept in a 12-hour light and dark cycle. They were water deprived for 12 hours each day before their behavioural training. Humidity (~55%) and temperature (~25°C) were well monitored.

Following were the various experimental and control groups:

1. Experimental: Enriched GAD2GluA2$^{\Delta ht}$ mice
2. Controls: a. Non-Enriched GAD2GluA2$^{\Delta ht}$ mice
   b. Enriched C57BL6J mice

All experimental procedures were approved by Institutional Animals Ethics Committee (IAEC), IISER Pune and Committee for the Purpose of Control and Supervision of Experiments on Animals (CPCSEA), Government of India.

2.2. Environmental Enrichment Chamber

The environmental enrichment chamber measured 90cm x 60cm x 40cm and was custom-made of Plexiglass (Figure 4). There are two levels in the set-up. The upper level is one-third in length as compared to the bottom one. The bottom level

contained two running wheels, tunnels, wooden hut, wooden chew toy and two toys covered with sandpaper of different grit size. Enough nesting material was also kept. Somatosensory stimulation was achieved when mice came in contact with the nesting material and the sandpaper. The running wheels were a source of physical exercise for the mice, possibly resulting in better motor abilities. There was a staircase (made of Lego ® blocks) to aid the mice traverse to the upper level whenever they wanted to access it. On the upper level, a maze was built using Lego® blocks. This maze was changed every week in order to stimulate the cognitive abilities of the mouse. Other than the maze, the upper level also consisted of a spinning wheel and another hut. There were eight ports to supply the chamber with the filtered air and keep it well-ventilated i.e., 4 inlets and 4 outlets. The enrichment chamber was cleaned every week. An important aspect of this paradigm was also olfactory enrichment with the help of natural odors. Thus 3 odor boxes were kept in the EE chamber (Table 2). The odors in these boxes were changed every alternate day.

Natural odors used in odor boxes	Cloves, chocochips, cinnamon, almonds, bay leaves, cardamom, coriander seeds, cumin, raisins

Table 2. Natural odors used in our EE paradigm.

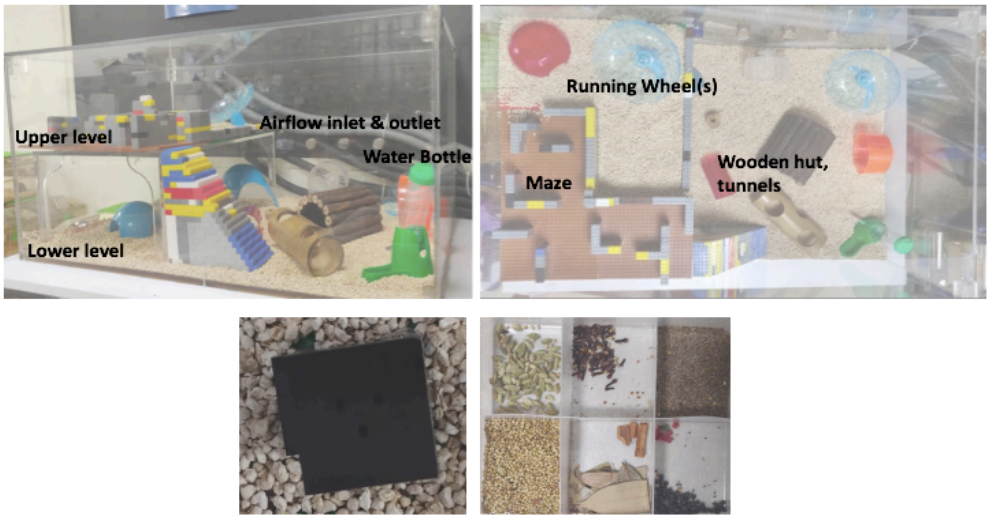

Figure 4. EE chamber.

(Upper Panel) The Environmental Enrichment chamber with all its constituents.

(Lower Panel) Odor boxes and the natural odors being used for olfactory enrichment.

2.3. Odors used

The following odors were used in the behavioral experiments:
Octanol+ (Oct+), Octanol- (Oct-), Hexanal (Hx), 3-Pentanone (Pn)
All odors were purchased from Sigma Aldrich. For the experiments, 1% dilution of odors was made in mineral oil. The mineral oil was bought from Oswal Pharmaceuticals (Pune).

2.4. Behavioral Paradigm: The go/no-go task

All behavioral training was performed on custom made Olfactometers which run on the Igor software (Wavemetrics, OR). The Olfactometer was used to do odor discrimination as well as airflow discrimination tasks. In a particular discrimination task, the mouse would be presented with two different stimuli (either odor or airflow). One of the stimuli, S+ (rewarded stimulus), is associated with a reward in the form of water. There is no reward or negative reinforcement for the other stimulus, S- (non-rewarded stimulus). Mouse is placed in an operant chamber with a combined sampling and reward port (Figure 5, left). A particular trial is initiated as the mouse pokes his snout inside the sampling port and breaks the infrared (IR) bream present there. This leads to opening of one of the odor valves and a final valve. The final valve diverts the airflow from the sampling area for 500 ms. This ensures quick odor delivery to the mouse. The mouse is then presented with either S+ or S- for a duration of 2 s (or 2000 ms) (Abraham et al. 2004, Abraham et al. 2010).

As a criterion for decision making, the total stimulus presentation time can be divided into 4 bins of 500 ms each. For a S+ trial to be correct, the mouse should lick at least once in three out of four bins. For a S- trial to be noted as a correct trial, mouse should not lick for more than two bins. In this paradigm, 3 to 4 such tasks are performed where each task consists of 300 trials. By the end of training, the mice learn to lick when presented with S+ and withdraw their snout/head when presented with S- stimulus. Airflow was delivered to mice through four tubes (4mm in diameter). As shown in Figure 5 (bottom), two tubes each were present on either side of the licking ports. Airflow is controlled with the help of flowmeters. An anemometer is used to initially measure the airflow. However, before the commencement of training, the mice underwent habituation. This pre-training

consists of eight phases. In the phase 0, the mouse gets water as a reward for simply inserting its head in the sampling port. Thus, the phases progress with an increase in the level of complexity such that Phase 8 resembles an actual training session.

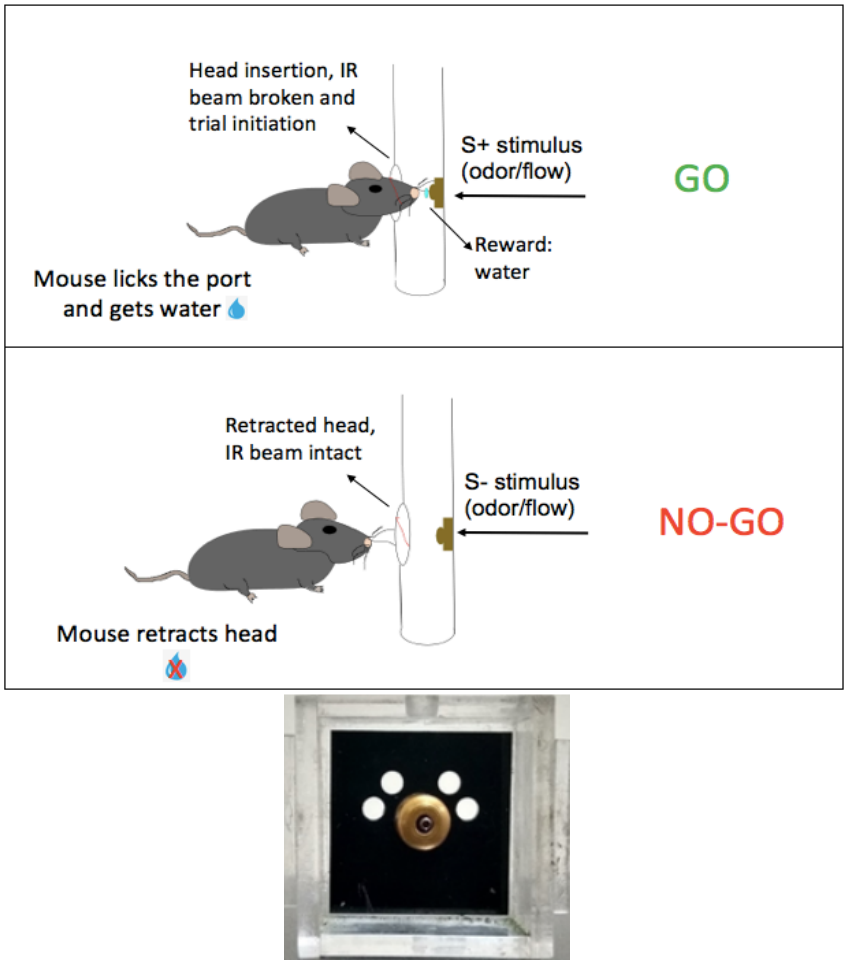

Figure 5. The go/no-go behavioral paradigm.
(top) The mouse is presented with a rewarded (S+) and non-rewarded stimulus (S-). It learns to lick for the S+ stimulus (Go) and retract its head for S- stimulus (No-go).
(bottom) Stimulus delivery chamber for airflow discrimination task.

Using the same paradigm, the memory of the mouse for particular odor pair can also be tested. If memory for an odor pair is to be checked, a Resistance to Memory Extinction (RME) task is performed after training for that odor pair is finished. In the RME task, 100 trials are performed: 50 of S+ and 50 or S- for which memory will be checked 30 days later. Out of the S+ trials, only half of them are rewarded as compared to all S+ trials being rewarded in the usual discrimination task. This is done to ensure that the mouse performs the task with greater attention and there is

delay in memory extinction. It is based on Bouton and Sunsay's "Partial Reinforcement Theory" (Bouton & Sunsay, 2001).

One month after the RME task, the memory task is performed. Before memory task, a background odor pair (different from the odor pair whose memory is to be tested) task is performed. During a memory task, mice are exposed to 200 trials of the background odor pair. Among the background trials, memory trials are also interspersed. The memory trials are not rewarded with water. There are four trials of memory odor pair in the 20 trial blocks making it a total of 28 memory trials (out of 200), checked over 7 blocks.

2.5. Readouts of the Behavioral Tasks

In order to gain a better understanding of the observed behavior during a particular odor or flow discrimination tasks, the following parameters are studied (Abraham et al., 2004):

- Learning efficiency: The accuracy (% correct) of the animal to carry out a trial of go/no-go odor discrimination task is evaluated as the training progresses. For example, at the beginning of task 1 the mouse might start with chance level accuracy of 50% which would increase as the trials progress. An average accuracy of 100 trials is plotted on the x-axis. Thus, this particular parameter gives insight about the learning pace of the mouse.

- Discrimination Time (DT): It is the time taken by the animal to discriminate between the S+ and S- stimuli and react by either licking for rewarded trial or retracting the head for a non-rewarded trial. Following are the methods to calculate DT:

  The *sample pattern* is calculated on the basis of the breaking of IR beam. Binary values are given to broken IR beam and an intact one. This is plotted against the duration of the stimulus (Figure 6A1). The total stimulus duration is divides into 125 time bins of 20 ms. For an S+ trial, the mouse would keep its head inside the sampling port, thus having high sampling percentage. In

case of S- trials, the mouse would retract its head quickly, leading to a decrease in sampling percentage. Log (p-value) plots for the difference between S+ and S- were plotted. The last point at which the curve crossed p=0.05 was chosen to be the DT. The first point since onset of stimulus where the reaction to S+ and S- significantly diverges ($p<0.05$) is called the discrimination time (DT).

The *lick pattern* is calculated using the licks, which are registered on the licking port. For a S+ trial, the mouse would lick for a longer duration, leading to an increase in licking percentage and for a S- trial, licking percentage would be less as the mouse would retract its head (Figure 6B1). Again, Log (p-value) plots for the difference between S+ and S- were plotted. The last point at which the curve crossed p=0.05 was chosen as the DT.

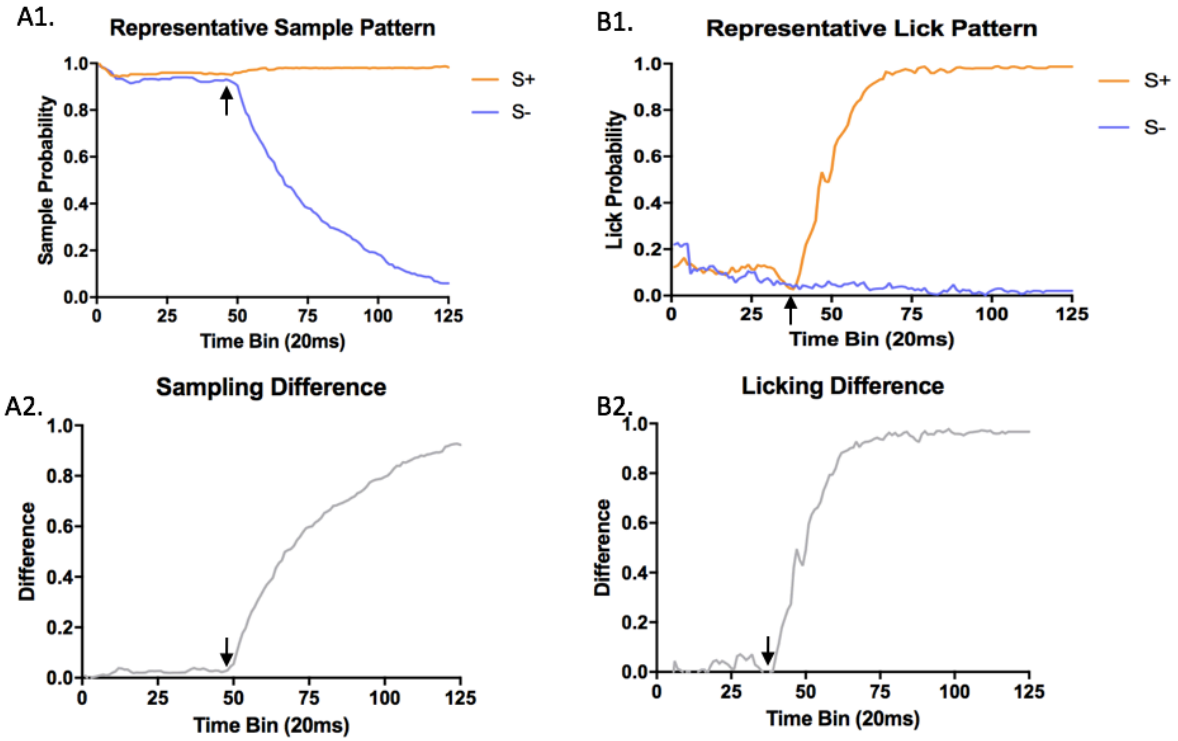

Figure 6. Calculation of Discrimination times. Sample pattern (A1) and Lick Pattern (B1) is used to calculate DTs. Once S+ and S- curves from A1 and B1 are obtained, their differences are plotted (A2 and B2). The last point at which the curve crossed p=0.05 was chosen to be the DT (shown by black arrow).

- Inter-Trial Interval (ITI): It refers to the time interval between two consecutive trials. This parameter is a readout of the animal's motivation to perform the

task. If the ITI is too long, the animal could be under-motivated to perform the task as its thirst could be quenched. If the ITI is too less and the mouse is repeatedly licking between the trials, then it could be a sign of over-motivation to lick on the tube in anticipation of water.

- Lick Percentage (% Licked): The percentage of time that the mouse spends licking during the stimulus duration is called the % licked. To obtain % licked, the time spent licking during the stimulus duration is divided by the total duration of the stimulus and multiplied by 100. To plot the % Licked, an average of all trials for all animals of a particular group is calculated. As the mouse starts with task 1, and cannot discriminate between the two stimuli accurately, it licks for both S+ and S-. Thus, lick percentage is very high. However, once the mouse is able to accurately discriminate between the two stimuli, it licks for S+ and doesn't lick for S-. The lick percentage decreases to almost chance level. Lick percentage is also a readout of the motivation of the mouse. A higher lick percentage would point towards over-motivation whereas a lower one might reflect under-motivation.

2.6. Transcardial perfusion & sectioning

Mice were anaesthetized using Thiopentone Sodium (Neon Laboratories, 50mg/kg). Following this, perfusion was carried out using 1x Phosphate Buffered Saline (PBS) and then 4% Paraformaldehyde (PFA, Sigma Aldrich). Finally, the head of the mouse was decapitated and the brain (with intact OB) was dissected. The brain was stored for a day in 4% PFA. One day before sectioning of the brain, it is kept in 30% sucrose solution. The brain is sectioned using a cryotome (Leica).

2.7. c-Fos Antibody staining on freely floating brain sections

A proto-onco gene, c-Fos is a marker for recent synaptic activity (Bullitt, 1990). For c-Fos analysis, 50µm thick horizontal sections were utilized. From each group, 4 animals were used for c-Fos staining. Thus, from each animal, 5 horizontal sections were present. Three washes (15 minutes/wash) of Tris-Buffered Saline were given. After each wash, the plate containing the sections was kept on the rocker. Blocking was done for one hour to remove any non-specific binding. The blocking solution consisted of 0.2% Triton-X (Sigma), 7.5% Normal Goat Serum(NGS) (Abcam,

ab7481) and 2.5% Bovine Serum Albumin (BSA) (Sigma Aldrich) in TBS. Following blocking, primary antibodies: rabbit anti-c-Fos (1:500 dilution) and chicken anti-NeuN (Millipore, ABN91) or anti-Map2 (1:1000) (Abcam, ab92434) dilution. The sections were incubated overnight at 4°C for 13-15 hours. The next day, again, three TBS washes (15 minutes/wash) were given. Then, secondary antibody incubation was done for two hours at room temperature. The secondary antibodies used were anti-rabbit Alexa Flour 594 (1:500 dilution) and anti-chicken Alexa Flour 488 (1:500 dilution) (Jackson Immunoresearch, USA, code:111-585-003 & 712-544-150) . Three TBS washes (15 minutes/wash) were given. Finally, the sections were put in DAPI (Sigma, 1:500 dilution in 1% NGS) for 10 minutes. Vectashield Anti-flour medium (Vector labs) was used to mount sections onto the glass slides (Methodology for immunostaining adapted from Pfarr et al., 2018).

2.8. BrdU Antibody staining on freely floating brain sections

Bromodeoxyuridine (BrdU) (TCI chemicals, dissolved in 0.9% saline solution) is a marker for proliferating cells. Three or four of the animals from each group were injected with BrdU 28-30 days before the perfusion day. Intraperitoneal injection was given to the mice 4 times a day at an interval of two hours. The dosage of BrdU injection was 100mg/kg (Gratzner, 1982).

Perfusions of the BrdU injected mice were carried out 28 days after the injections. Coronal sections of OB, which were 50 µm thick, were taken using cryotome. For immunostaining, sections at 300 µm difference were chosen. Thus, for each OB of a mouse, 7-9 sections were used. Sections were given three PBS washes (15minutes/wash). Then, the sections were put in 1N hydrochloric acid (HCl) and kept in incubation at 37°C in a thermoshaker (Eppendorf) for 45 minutes. Following this, three PBS washes were again given (15 minutes/wash). Sections were kept in the blocking solutions for two hours. The blocking solution consisted of 5% NGS (Abcam, ab7481) and 1% Triton-X (Sigma) in PBS. After that, primary antibody incubation was done for 22 hours. The primary antibodies used were rat anti-BrdU (1:1000 dilution) (Biorad, MCA2060) and chicken anti-Map2 (1:500 dilution) (Abcam, ab92434). After primary antibody incubation, three PBST (0.3% Triton-X in PBS) washes were given. Sections were also washed with PBS once (15 minutes/wash).

Secondary antibody incubation was done for 2 hours. The secondary antibodies used were anti-rat Alexa Flour 488 (1:500 dilution in 1% NGS) and anti-chicken Alexa Flour 647(1:500 dilution in 1% NGS) (Jackson Immunoreach, USA, 712-544-150 & 703-605-155). Finally, DAPI was added to the sections (1:500 dilution in 1% NGS) (Sigma) for 10 minutes. Vectashield Anti-flour medium (Vector labs) was used to mount sections onto the glass slides.

2.9. Imaging and Analysis

c-Fos imaging and quantification: Imaging for c-Fos sections was performed on a Leica sp8 confocal microscope. For each horizontal section, the following layers or regions were imaged in a z-stack: Glomerular Layer (GL), Mitral Cells (MCs), Granule Cell Layer (GCL) and the Anterior Olfactory Nucleus (AON). For GL, MCL and GCL, four z-stack images each (per OB) were taken at random in one section. In case of AON, ~4-6 field of view were imaged per section. Imaging was performed at 40x. Co-localization of c-Fos positive (c-Fos+) cells was checked with DAPI positive (DAPI+) cells. In order to calculate the number of co-localizing c-Fos+ cells, Imaris software was used. Mander's co-efficient A and B was also studied to gain insight about the extent of co-localization between DAPI+ and c-Fos+ cells in a particular region of interest.

BrdU imaging and quantification: Imaging to investigate BrdU positive (BrdU+) cells was also performed using a Leica sp8 confocal microscope. For each of the 8-9 coronal OB sections per animal, 10x z-stack images were taken. The number of BrdU+ cells were calculated using the Fiji ImageJ software. A plugin called 'Analyze Particles' was used.

2.10. Photoionization Detector (PID)

A Fast-Response Miniature Photo-Ionization detector (PID) (Aurora Scientific Inc.) was used to measure odor concentration when the flow is presented to animals during airflow discrimination tasks. A PID is an instrument which is capable of measuring the concentration of gases and various volatile organic compounds. Ultraviolet light is used by this instrument in order to ionize the odor or gas sample. The PID analysis chamber contains two plates that create a difference in potential.

Thus, as the ionized molecules reach this chamber, a current is created and recorded.

Greater concentration of odor would imply a greater number of ionized molecules and thus, a greater intensity of current (Bax et al.,2020). So, as an odor reaches the detector, a peak would be expected whose amplitude would vary from odor to odor depending on properties like odor concentration and vapor pressure.

In the PID experiments performed, an average of measurements of 15 trials were taken for each airflow and odor condition. The data is plotted for a total of 3000ms, 500ms before and 500ms after stimulus delivery. The stimulus delivery duration is 2000ms.

2.11. DNA Extraction & Polymerase Chain Reaction (PCR)

Genotyping of GAD2GluA2$^{\Delta ht}$ mice was also performed for GAD2 and GluA2 to confirm that the mice were indeed heterozygous. First, DNA extraction was carried out from tail clippings of mice.

For each piece of tail placed in an Eppendorf tube (1.5 mL), 80 µL of PCR grade water (Sigma-Aldrich), 12 µL of express extract buffer (KAPA Biosystems) and 2 µL of extract enzyme (KAPA Biosystems) was added. The tail clipping was completely immersed in this solution. A dry bath was given to the samples at 75°C for 15 minutes. Immediately afterwards, samples were placed in another dry bath at 95°C for 10 minutes. The samples were put in a centrifuge (Thermo Scientific) at 4°C for 5 to 7 minutes (at 10,000 RPM). Finally, the supernatant (around 70 µL in volume) was collected and stored in 4°C for further use.

Next, PCR reactions were carried out using C1000 Touch^{TM} Thermal Cycler (Biorad).
The following ingredients were added to the reaction mix:

- PCR grade water (Sigma-Aldrich)
- Express extract buffer (KAPA Biosystems)
- 25mM Magnesium Chloride ($MgCl_2$) (KAPA Biosystems)

- 10mM KAPA Deoxynucleoside Triphosphates (dNTP) mix (KAPA Biosystems)
- Forward and Reverse Primers (Sigma-Aldrich)
- Taq Polymerase enzyme: 50U/µL KAPA 2G Fast Hot Start (KAPA Biosystems)

Primers used:

For GAD2 characterization,

- 19048 (forward): 5'- CACTGCATTCTAGTTGTGGTTTG-3'
- 28223 (reverse): 5'-TCGTTGCACTGACGTGTTCT-3'
- 28224(reverse): 5'-AACAGTTTGATGAGTGAGGTGA-3'

For GluA2 characterization,

- VM10 (forward): 5'-GTTGTCTAACAAGTTGTTGACC-3'
- VM12 (reverse): 5'-GCGTAAGCCTGTGAAATACCTG-3'
- VM17 (reverse): 5'-GAATCATTGTTGACAGATTGCCAC-3'

The possible band sizes are:

In case of GAD2, Mutant = 176bp, Heterozygous = 176bp & 225bp, Wild Type = 225bp

In case of GluA22, Mutant = 254bp, Heterozygous = 254bp & 321bp, Wild Type = 321bp

Thus, PCR reactions were set with the following cycling conditions:

GAD2	GluA2
Initial Denaturation: 94°C for 2 mins Denaturation: 94°C for 20 secs Annealing Temperature: 65°C for 15 secs (-0.5°C/cycle) Extension: 68°C for 10 secs (10x) Denaturation: 94°C for 15 secs Annealing Temperature: 60°C for 15 secs Extension: 72°C for 10 secs (28x) Final Extension: 72°C for 2 mins	Initial Denaturation: 94°C for 2 minutes Denaturation: 94°C for 30 secs Annealing Temperature: 54.4°C for 30 secs Extension: 72°C for 50 secs (35x) Final Extension: 72°C for 2 mins

Table 3. PCR cycling conditions for GAD2 and GluA2

As observed in Figure 7A1, both the PCR gel images contain 2 bands for GAD2 mice, at 176bp and 225bp. This implies that the animals are heterozygous. A similar case is observed for GluA2 (Figure 7A2) where two heterozygous bands are found at 321bp and 254bp.

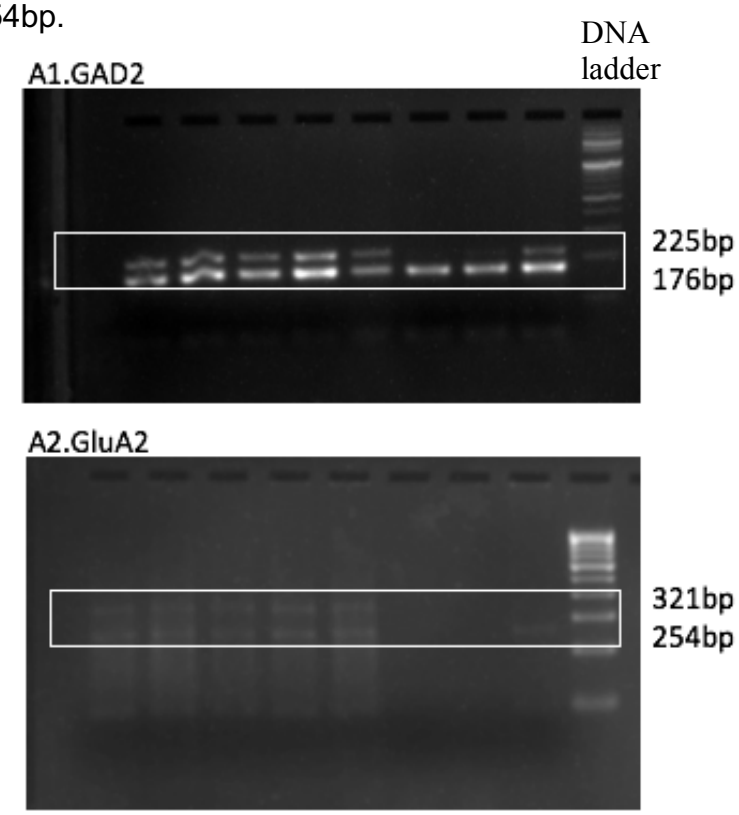

Figure 7. PCR gel image for:

A1. GAD2 and

A2. GluA2

Note: Each lane in the PCR gel image represents the genotyping of an individual GAD2GluA2$^{\Delta ht}$ mouse. Thus, genotyping for nine mice was performed, as shown above. The DNA ladder is loaded on the extreme right well.

3. Results

3. 1. Validating absence of odorant molecules during airflow discrimination tasks

Even though *in-vitro* studies allude that olfactory system is capable of sensing both chemical as well as mechanical information (Minghong Ma, 2009), *in-vivo* evidence needs to be further explored. Our experiments, investigating the effect of EE on airflow information processing, involved carrying out go/no-go behavioral training which, consisted of airflow and odor discrimination tasks. In order to investigate the airflow discrimination abilities of the mice, it had to be ensured that the mice were presented with nil/minimal odorant molecules particularly during the airflow discrimination training. Room air was pumped in the olfactometers for delivering different airflow rates to the mice. PID measurements were carried out to ensure the absence of any major odorous molecules in the air. As observed in the PID plots for various flows (Figure 8A to 8F), we do not observe any small changes in the voltage of signal during the stimulus duration, indicating the absence of odor molecules (as compared to PID measurements for odors in Figure 9).

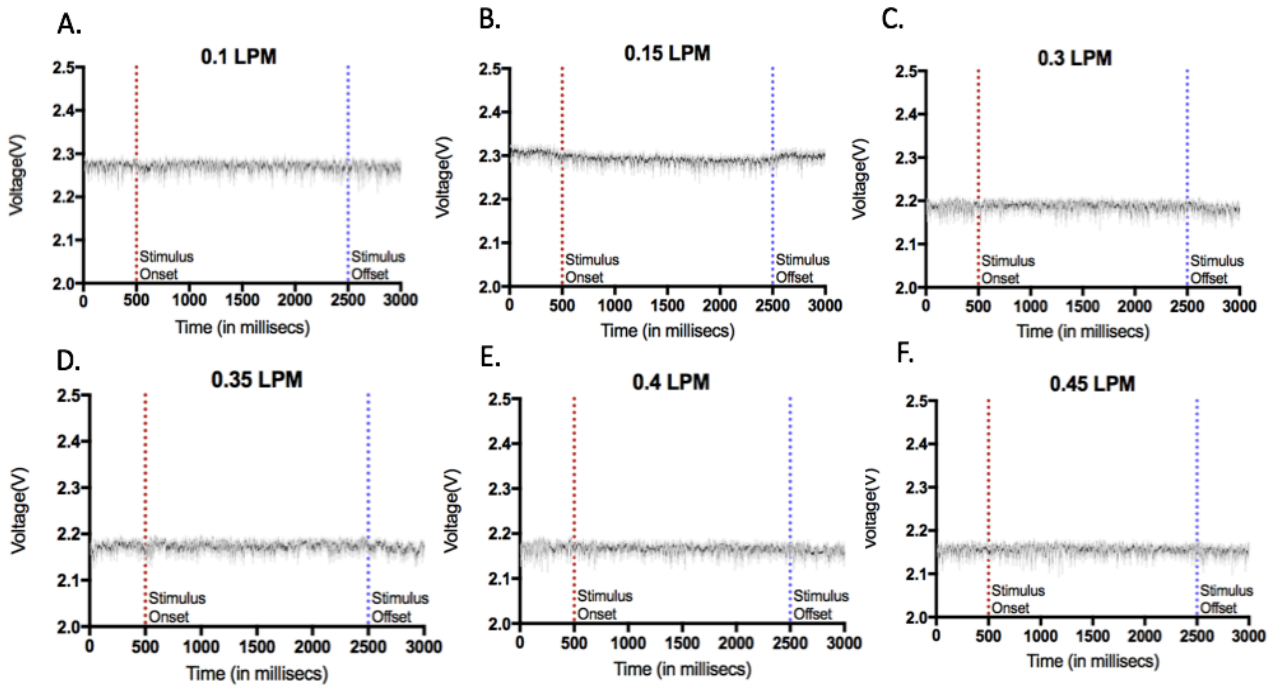

Figure 8. PID plots for airflow experiments. PID measurements for various airflow rates confirms the absence of odor molecules during airflow discrimination task. X axis represents stimulus duration (in millisecs) whereas Y axis represents Voltage (in

Volts). The red dotted line signifies the stimulus onset while the blue dotted line denotes the stimulus offset. The plots also have the PID measurements for before as well as after (500 ms each) the stimulus duration (of 2000ms). Throughout the three regions: before, during and after stimulus duration, no changes in the voltage are observed. The gray region represents the SEM. A-F. PID experiment was performed along with Sarang Mahajan, LNCB.

In order to compare the airflow presentation (during airflow discrimination task) to odor presentation (during odor discrimination tasks), PID measurement was also done for various odors used during the task. It was verified that the odors that we used at a specific dilution and flow-rate were indeed detectable. This experiment was carried out for the odors which were used in odor discrimination and odor coupled with flow discrimination tasks. All four PID plots show change in voltage (Figure 9 A-D). Thus, minimal presence of odorants during an airflow discrimination task and sustained presence of odor molecules during the stimulus duration time window in an odor discrimination task was confirmed.

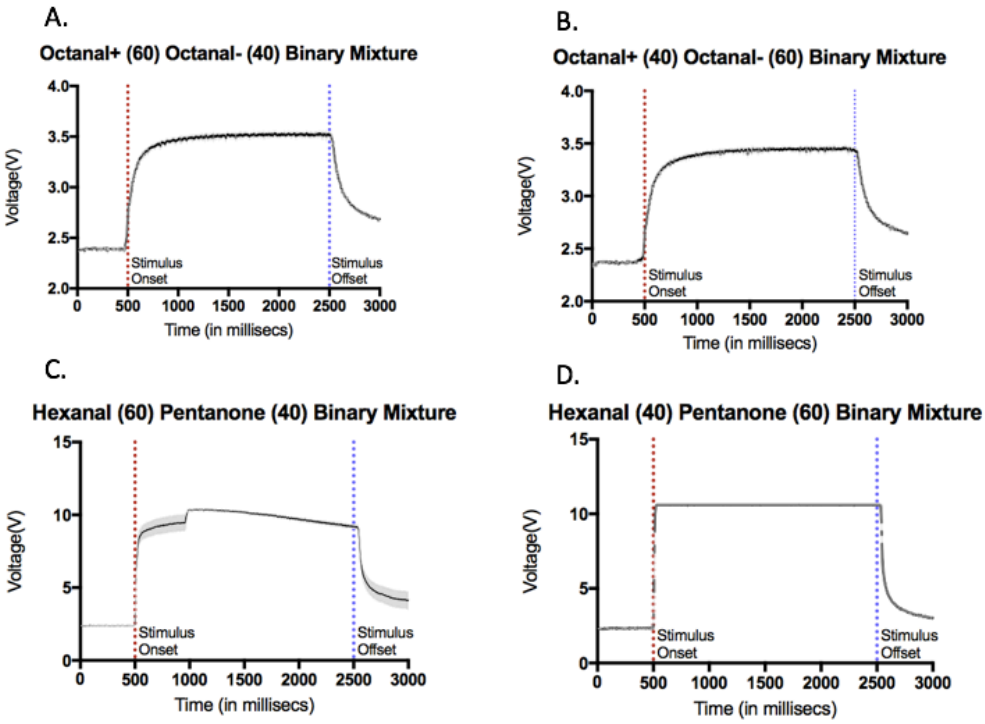

Figure 9. PID plots for odor and odor coupled with flow experiment verified that odors used are detectable. X axis represents stimulus duration (in millisecs) whereas Y axis represents Voltage (in Volts). For the PID experiments, 1% dilution of the odors was prepared in mineral oil. The red dotted line signifies the stimulus onset while the blue dotted line signifies the stimulus offset. The plots also have the PID

measurements for before as well as after (500 ms each) the stimulus duration (of 2000ms).

(A *& B) PID plot for Octanol (+/-) Binary Mixture (used in odor discrimination task)*

(C & D) PID plot for Hexanal and Pentanone Binary Mixture. These two plots have been calculated at 0.4 LPM and 0.3 LPM as they have been coupled with these airflows in the odor coupled with flow experiment. PID experiment was performed along with Sarang Mahajan, LNCB. The gray region represents the SEM

Note: Y-axis is varying across (A.B) and (C.D) because of different vapor pressure (for different odors). Also, mixing of odors leads to changes in its ionization properties.

To confirm the nil/minimal presence of odorant molecule, mice were trained for 300 trials on a control task where both the S+ and S- stimulus was 0.6 LPM. This particular experiment was performed after two airflow discrimination experiments. As expected, all mice groups had a chance level performance of around 50% in this task (See Supplementary Information, Figure S1). These results also confirmed that mice were using only the airflow rate differences as the cues, but not any unintended cues such as clicking noises of airflow stimuli delivery valves. In another experiment performed in the lab (by Sarang Mahajan, LNCB) mice were trained for the above-mentioned task with the air delivered from the air cylinder (gas composition was 20.5% Oxygen in Nitrogen and gas impurities were less than 1 ppm of hydrocarbons and less than 5ppm of moisture) and they showed chance level performance. But, the same mice learned to discriminate different airflow rates with the high accuracy while trained with the same air delivery system (Not shown here).

3. 2. Environmental enriched housing leads to the rescue of airflow discrimination learning deficits in GAD2GluA2$^{\Delta ht}$ mice

To study the effect of EE on airflow rate based learning in GAD2GluA2$^{\Delta ht}$ mice, three groups of mice: Enriched GAD2GluA2$^{\Delta ht}$, Non-Enriched GAD2GluA2$^{\Delta ht}$ and Enriched C57BL6/J (wild type), were utilized. They were weaned on Post-Natal Day (PND) 28. When the mice were 6-8 weeks old, they were either shifted to the EE chamber or a standard housing cage. This was followed by two weeks of either EE cage or

Standard Cage exposure without conducting any experimental procedures. At the end of two weeks, pre-training (also called the detection task) of the animals was started. This detection task was followed by a series of Go/No-Go flow/odor discrimination as well as olfactory memory tasks. Mice were initially trained to discriminate between flow-only pairs (0.35 vs 0.45 LPM and 0.1 vs 0.15 LPM) and odor-only pair (Octanal (+/-) binary mixture). After that, the two stimuli, odor and airflow were coupled for a discrimination task (Hexanal and Pentanone binary mixture, S+= 0.4 LPM, S-= 0.3 LPM). Once the behavioral experiments were over, mice were perfused. The brains were sectioned and immunohistochemistry for c-Fos and BrdU was carried out. The enriched mice were continued to be housed in EE cage until they were perfused. Finally, imaging for c-Fos (to check recent synaptic activity) and BrdU (to investigate OB adult neurogenesis) was performed using a confocal microscope. The details of the experimental timeline followed for the three groups of mice are as mentioned in the Figure 10.

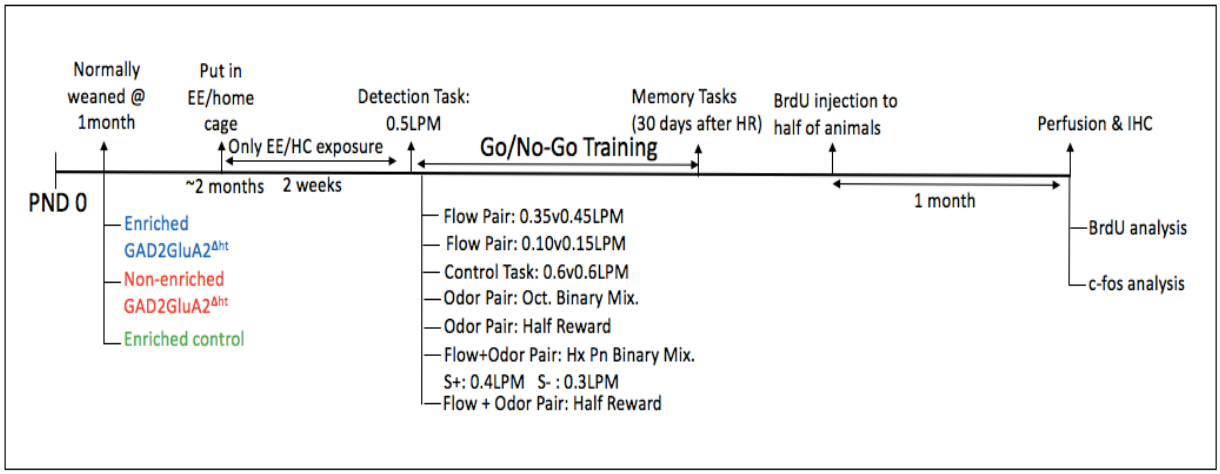

Figure 10. Timeline of the experiments performed. Three groups of mice were weaned when they were one month old. EE or home cage exposure was provided to mice for two weeks when they were 2 months old. Flow/Odor discrimination training was carried out followed by perfusion of animals. Finally, BrdU and c-Fos staining was performed. Note: Enriched mice were housed in EE chamber for the whole duration of the experiments until perfused.

It has been observed that GAD2GluA2$^{\Delta ht}$ mice show deficits in airflow information processing (Unpublished Data, Suhel Tamboli, Shruti Marathe, LNCB). They are unable to accurately discriminate between two different airflow rates. To investigate

whether GAD2GluA2$^{\Delta ht}$ mice indeed have airflow discrimination deficits and whether a rescue is possible through EE exposure, three groups of mice were trained to discriminate between the airflow rates, 0.35 and 0.45 liters per minute (LPM). In previous experiments (performed by Sarang Mahajan, LNCB), it has been observed that 0.35 LPM and 0.45 LPM lie within the perceptual range for airflows for wild-type mice, i.e. mice are able to discriminate between these two airflow rates. The same is also true for 0.1 LPM and 0.15 LPM (which is the airflow discrimination task that was performed next). In order to habituate to the chamber and get familiarized with the Go/No-Go paradigm, mice had to undergo pre-training, which consisted of eight phases. After each mouse completed the eight phases, (see methods), 0.35 vs. 0.45 LPM discrimination task was carried out. The non-enriched GAD2GluA2$^{\Delta ht}$ mice were unable to accurately discriminate between the two airflow rates and their accuracy remained at the chance-level. By the end of task 4, i.e. 1200 trials, the non-enriched GAD2GluA2$^{\Delta ht}$ mice reached an accuracy of only 56% (See Supplementary Information, Figure S2). Another set of GAD2GluA2$^{\Delta ht}$ mice that were continually exposed to EE, were able to discriminate between the two airflows and ended the last task with an average accuracy of 91%. The enriched wild-type group was also significantly better at 0.35 vs 0.45 LPM discrimination as compared to the non-enriched GAD2GluA2$^{\Delta ht}$ group and had the same learning pace as enriched GAD2GluA2$^{\Delta ht}$ mice. Thus, after exposure to an enriched environment, GAD2GluA2$^{\Delta ht}$ mice perform as accurately as enriched wild-type mice (Figure 11A1**,** Two-way ANOVA, $p<0.0001$ $F=777.2$, Tukey's Test).

Further, we investigated the discrimination times (DTs) shown by the animals to gain insight into the observed airflow discrimination deficit in GAD2GluA2$^{\Delta ht}$. DT is the time taken by the animal to discriminate between the S+ and S- stimulus. Thus, DT measurements (from the lick pattern and the sample pattern) were also compared for all three groups of mice for 0.35 vs 0.45 LPM discrimination. In case of DT which was measured using sample pattern, the non-enriched GAD2GluA2$^{\Delta ht}$ mice were significantly slower (1584ms) than both the other groups (Figure 11A2**,** Ordinary One-way ANOVA, $p<0.0001$ $F=65.79$, Tukey's test). There was no statistical difference between the DT of the enriched GAD2GluA2$^{\Delta ht}$ mice and the enriched wild-type mice. A similar trend was also observed when DT measurements were calculated using the lick pattern (Figure 11A3**,** Ordinary One-way ANOVA, $p<0.0001$

F=47.43, Tukey's test). The non-enriched GAD2GluA2$^{\Delta ht}$ mice had a DT of 1606ms which was significantly slower than both enriched GAD2GluA2$^{\Delta ht}$ mice (381ms) and the enriched wild-type mice (352ms).

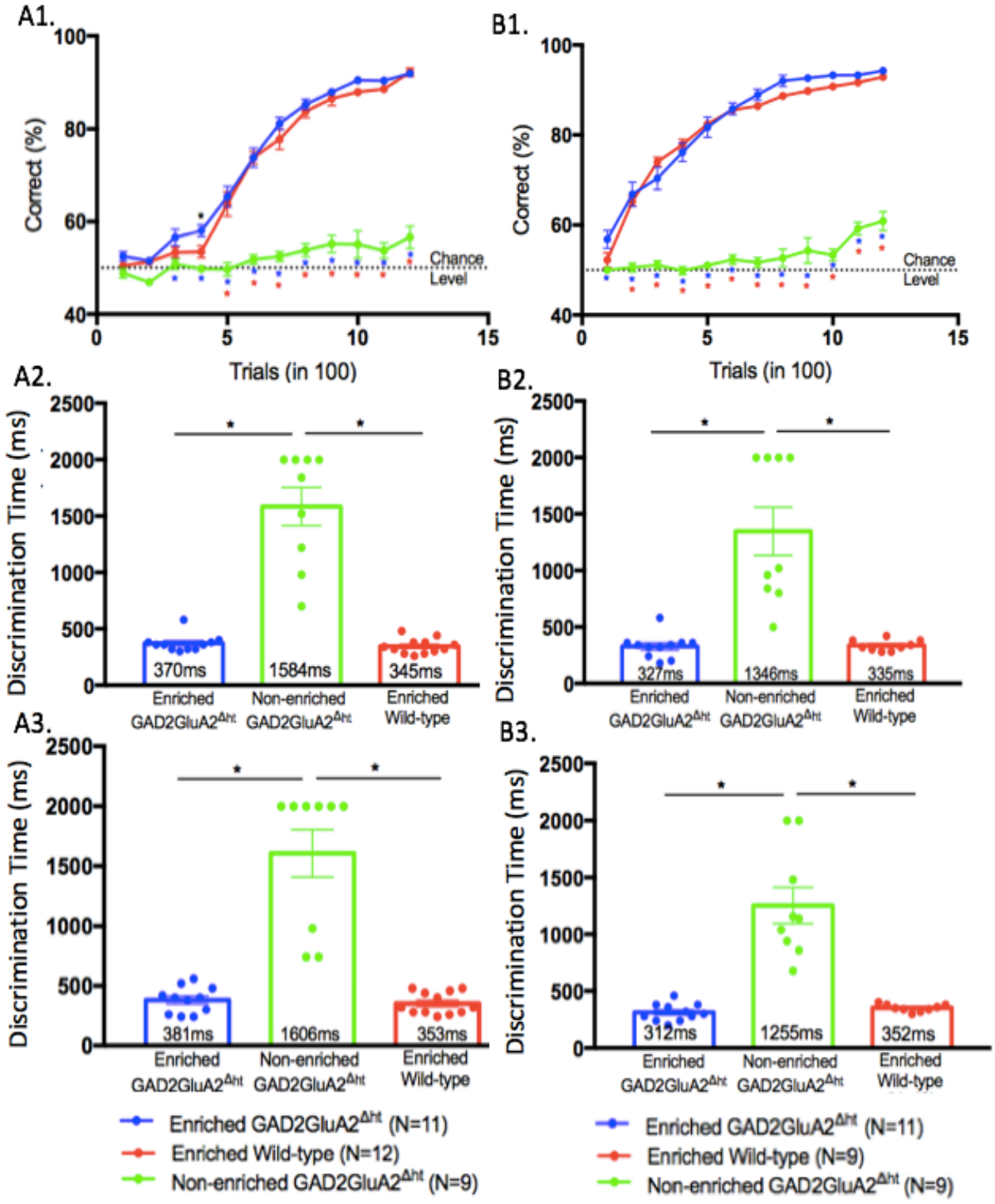

Figure 11. Rescue of airflow discrimination deficits observed in GAD2GluA2$^{\Delta ht}$ mice after EE exposure. (A1-A3) 0.35 vs 0.45 LPM.

*(A1) Learning efficiencies, where X-axis represents trials (averaged over 100 trials) and Y-axis represents the accuracy in % (Two-way ANOVA, p<0.0001 F=777.2, Tukey's Test, * p<0.05 for Non-enriched GAD2GluA2$^{\Delta ht}$ mice vs Enriched GAD2GluA2$^{\Delta ht}$ mice, * p<0.05 for Non-enriched GAD2GluA2$^{\Delta ht}$ mice vs Enriched wild-type mice * p<0.05 for Enriched GAD2GluA2$^{\Delta ht}$ mice vs Enriched wild-type mice). Each circle in the learning curve represents mean accuracy of 100 trials across all animals of that group. The error bars represent the SEM.*

*(A2) DT using sample pattern (Ordinary One-way ANOVA, p<0.0001 F=65.79, Tukey's test, *p<0.0001). Each circle represents the DT of an individual animal. The bar represents the mean DT of all animals of that group for the last task. The error bars represent the SEM.*

*(A3) DT using lick pattern (Ordinary One-way ANOVA, p<0.0001 F=47.43, Tukey's test, *p<0.0001). Each circle represents the DT of an individual animal. The bar represents the mean DT of all animals of that group for the last task. The error bars represent the SEM.*

(B1-B3) 0.1 vs 0.15 LPM.

*(B1) Learning curve (Two-way ANOVA, p<0.0001 F=1597, Tukey's Test *p<0.05, *p<0.05. Each circle in the learning curve represents mean accuracy across all animals of that group. The error bars represent the SEM.)*

*(B2) DT using sample pattern (Ordinary One-way ANOVA, p<0.0001 F=36.75, Tukey's test, *p<0.0001). Each circle represents the DT of an individual animal. The bar represents the mean DT of all animals of that group for the last task. The error bars represent the SEM.*

*(B3) DT using lick pattern (Ordinary One-way ANOVA, p<0.0001 F=24.72, Tukey's test, *p<0.0001). Each circle represents the DT of an individual animal. The bar represents the mean DT of all animals of that group for the last task. The error bars represent the SEM.*

To ascertain the ameliorating role of EE in governing the airflow discrimination abilities of GAD2GluA2$^{\Delta ht}$ mice, a second airflow discrimination experiment was performed. In this experiment, mice were challenged to discriminate between 0.1 LPM and 0.15 LPM. It was again observed that both the enriched group of mice learnt to discriminate between the two airflows at a significantly faster rate as compared to non-enriched GAD2GluA2$^{\Delta ht}$ mice (Figure 11B1, Two-way ANOVA,

p<0.0001 F=1597, Tukey's Test). By the end of task 4, while the enriched GAD2GluA2$^{\Delta ht}$ mice reached an accuracy of 93%, the non-enriched GAD2GluA2$^{\Delta ht}$ mice had a significantly lower accuracy of only 57% (See Supplementary Information, Figure S3). The learning pace of enriched GAD2GluA2$^{\Delta ht}$ mice and enriched wild-type mice was highly similar. The DT measurements had the same trend as the first flow pair. As compared to non-enriched GAD2GluA2$^{\Delta ht}$ and enriched wild-type group, the lick pattern and sample pattern DTs were significantly much higher in case of non-enriched GAD2GluA2$^{\Delta ht}$ mice (Figure 11B2**,** Ordinary One-way ANOVA, p<0.0001 F=36.75, Tukey's test; B3 Ordinary One-way ANOVA, p<0.0001 F=24.72, Tukey's test).

The inter-trial interval (ITI) and the percentage lick (% Lick) are the parameters controlled by the mice which give a readout of their motivational and arousal levels (Abraham et al., 2004). The percentage of time spent licking during the stimulus duration is represented by the % licked. The time between two consecutive trials is the ITI. In order to ensure that the differences observed in the learning efficiency and DTs between the enriched and non-enriched groups were not influenced by the motivational state of the mice, ITI and the % Lick were calculated for the last task (Task 4). As observed in Figure 12. (Ordinary One-way ANOVA, p>0.05, Tukey's Test), all values of ITI as well as % Lick for all three group were similar to each other. Thus, the behavioral readouts, accuracy of learning and DTs were not altered by the motivation and arousal state of the mice.

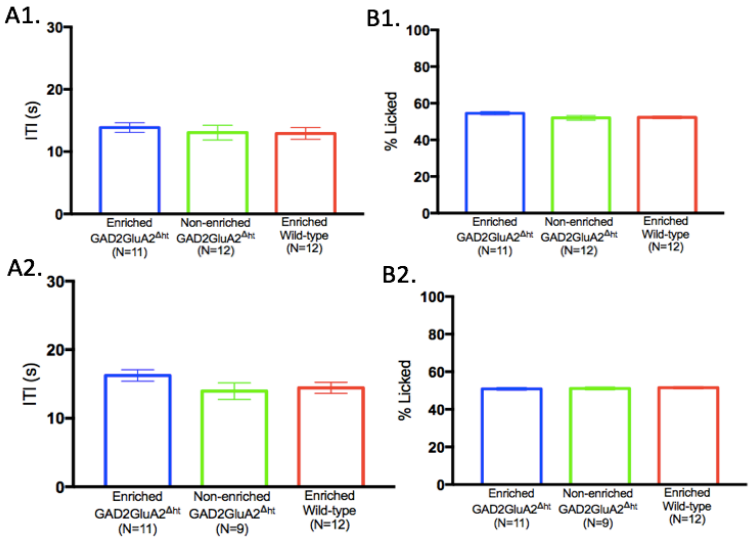

Figure 12. Motivation levels of the mice did not affect the observed results.

(A1) ITI for 0.35 vs 0.45 LPM (Ordinary One-way ANOVA, p=0.1944 F=1.741, Tukey's test). Each bar represents the mean ITI across animals of that group. The error bars represent the SEM.
(A2) % Licked for 0.35 vs 0.45 LPM task (Ordinary One-way ANOVA, p=0.1238 F=2.247, Tukey's test). Each bar represents the mean % Licked across animals of that group. The error bars represent the SEM.
(B1) ITI for 0.10 vs 0.15 LPM task (Ordinary One-way ANOVA, p=0.7458 F=0.2967, Tukey's test). Each bar represents the mean ITI across animals of that group. The error bars represent the SEM.
(B2) % Licked for 0.10 vs 0.15 LPM task (Ordinary One-way ANOVA, p=0.7936 F=0.2333, Tukey's test). Each bar represents the mean % Licked across animals of that group. The error bars represent the SEM.

Therefore, from the two airflow discrimination tasks that we conducted, it can be concluded that GAD2GluA2$^{\Delta ht}$ mice show learning deficits in airflow discrimination tasks. However, GAD2GluA2$^{\Delta ht}$ mice housed in an EE setting showed rescue of deficits in airflow rate based discrimination tasks and performed as well as wild-type mice housed in EE setting.

3. 3. Environmental enrichment housing leads to faster learning pace for odor discriminations

It has been observed that selectively knocking out GluA2 from GCs of OB leads to a faster discrimination time for distinguishing complex odor mixtures (Abraham et al., 2010). Thus, in order to consider a possible effect of GAD2 specific heterozygous GluA2 knockout on odor discrimination, mice were trained to discriminate Octanol (+/-) Binary Mixture. Three tasks of 300 trials each were performed. Unlike flow discrimination tasks, non-enriched GAD2GluA2$^{\Delta ht}$ mice were able to discriminate between these two odors with a good accuracy (89% by the end of Task 3) (Figure 13A1 Ordinary One-way ANOVA, p=0.1944 F=1.741, Tukey's test). However, as compared to the learning pace of the two enriched groups, the non-enriched were still slower as seen by their pace in the second task. Thus, EE was indeed leading to a faster learning pace for odor discriminations. There was no statistically significant

difference between the three groups when the lick pattern (Ordinary One-way ANOVA, p=0.6349 F=0.4623, Tukey's test) and sample pattern (Ordinary One-way ANOVA, p=0.1485 F=2.054, Tukey's test*)* DTs were analysed (Figure 13A2-A3). All DT measurements across groups were comparable and in the range of 300-410ms. Finally, ITI and % Licked were found to be also similar across all groups. Thus, motivation levels of the mice did not bring about changes in the observed behavior (Figure 13A4-A5).

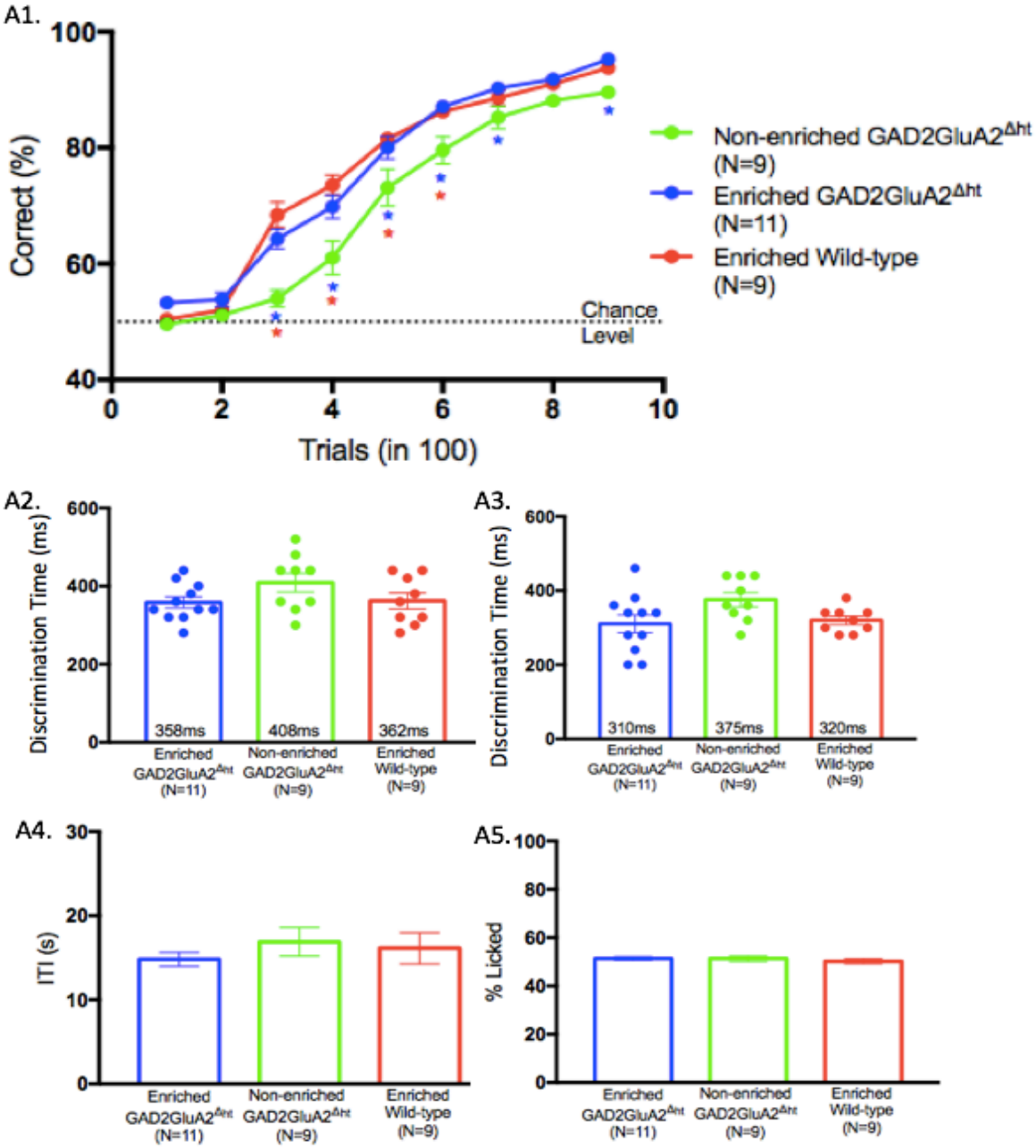

*Figure 13. Faster learning pace observed for odor discriminations (*Octanols (+/-)*) due to EE in GAD2GluA2$^{\Delta ht}$ mice and Wild-type mice.*

*(A1) Learning efficiencies (Two-way ANOVA, p<0.0001 F=46.42, Tukey's Test *p<0.05, *p<0.05). Each circle in the learning curve represents mean accuracy of 100 trials across all animals of that group. The error bars represent the SEM.*
(A2) DT using sample pattern (Ordinary One-way ANOVA, p=0.1485 F=2.054, Tukey's test). Each circle represents the DT of an individual animal. The bar represents the mean DT of all animals of that group for the last task. The error bars represent the SEM.
(A3) DT using lick pattern (Ordinary One-way ANOVA, p=0.0655 F=3.033, Tukey's test). Each circle represents DT of an individual animal. The bar represents mean DT of all animals of that group for the last task. The error bars represent the SEM.
(A4) ITI (Ordinary One-way ANOVA, p=0.5840 F=0.5438, Tukey's test). Each bar represents the mean ITI across animals of that group. The error bars represent the SEM
(A5) % Licked (Ordinary One-way ANOVA, p=0.6349 F=0.4623, Tukey's test). Each bar represents the mean % Licked across animals of that group. The error bars represent the SEM

3. 4. Environmental enrichment housing leads to faster learning pace during flow and odor coupled discrimination

Our results suggest that environmental enrichment leads to rescue of airflow discrimination deficits and a faster pace of learning during odor discrimination task. What would be the effect of enrichment on a task where both these stimuli are combined? It is possible that multisensory enhancement occurs and the presence of both odor and airflow as stimuli would lead to better learning. Multisensory enhancement has been explored more in sensory systems like auditory system or visual system. Since olfactory system is also involved in airflow information processing, whether both odor and airflow information would enhance the OB response remains elusive. Another possibility is that one of the cues can dominate the decision making ability of mice. In order to test these possibilities, a behaviour task was performed which consisted of a flow pair coupled with an odor pair. A binary mixture of Hexanal and Pentanone was used as the odor pair. The coupled flow pair was 0.4LPM (S+) and 0.3 LPM (S-). All the three groups of mice were able

to accurately discriminate between the flow and odor coupled pair (Figure 14A1). However, both the enriched groups were able to discriminate between the two stimuli at a much faster pace (Two-way ANOVA, p<0.0001 F=178.8, Tukey's Test *p<0.05, *p<0.05, *p<0.05). The enriched groups had a very fast learning pace and had reached almost 80% accuracy by the end of Task 1 itself. There was no statistical significance between the groups when the sample pattern DT (Ordinary One-way ANOVA, two-tailed, p=0.5515 F=0.6094) and lick pattern DT (Ordinary One-way ANOVA, two-tailed, p=0.0993 F=2.536) was compared. Motivational levels are not modulating the behavioral readouts as the ITI and the Lick % is comparable across the groups (Figure 14A4-5).

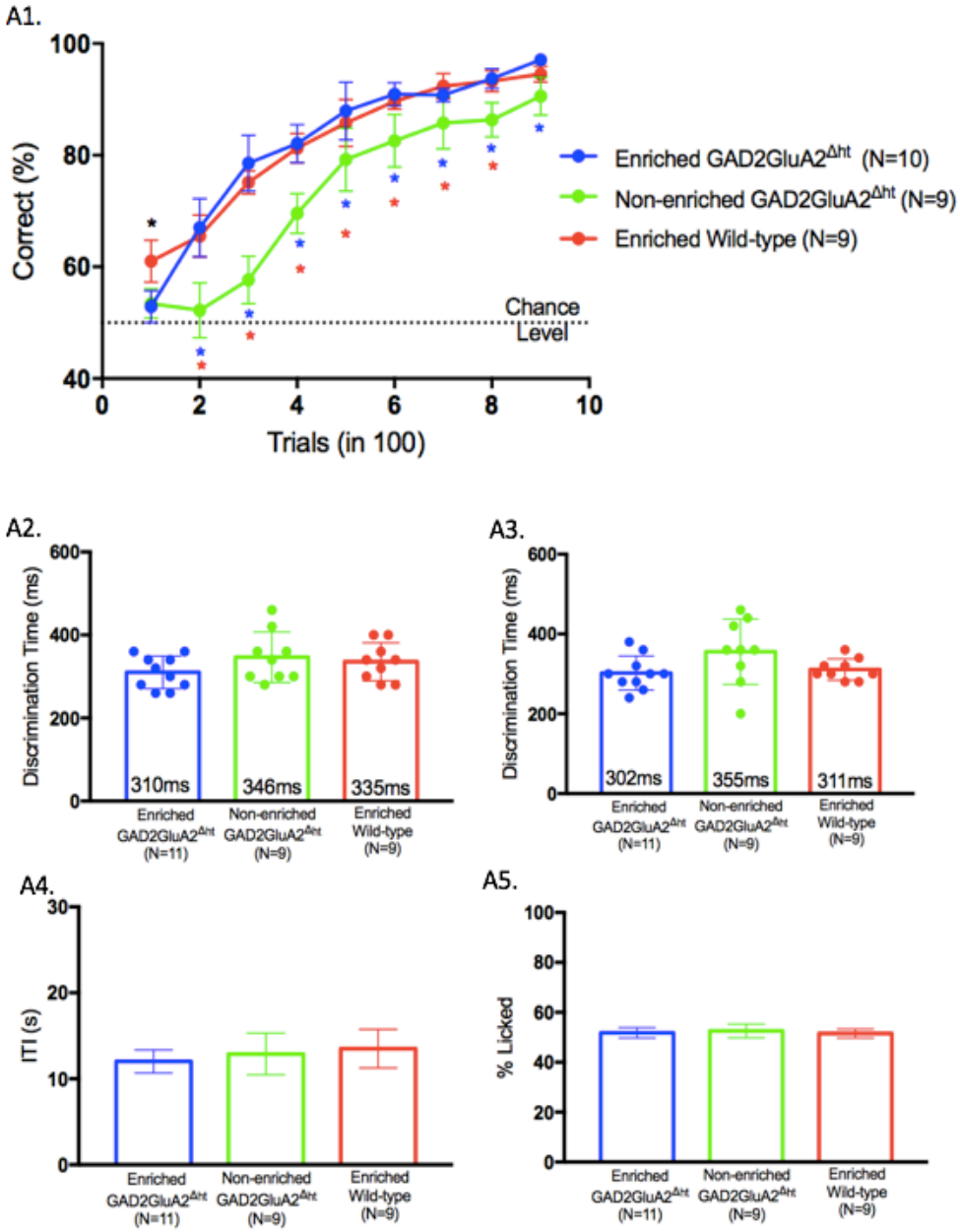

Figure 14. Faster learning pace was observed in a Flow pair coupled with odor discrimination task due to EE in GAD2GluA2$^{\Delta ht}$ mice and Wild-type mice.

(A1) *Learning efficiencies (Two-way ANOVA, p<0.0001 F=178.8, Tukey's Test *p<0.05, *p<0.05, *p<0.05), Each circle in the learning curve represents mean accuracy of 100 trials across all animals of that group. The error bars represent the SEM.*

(A2) DT using sample pattern (Ordinary One-way ANOVA, two-tailed, p=0.5515 F=0.6094), Each circle represents the DT of an individual animal. The bar represents the mean DT of all animals of that group for the last task. The error bars represent the SEM.

(A3) DT using lick pattern (Ordinary One-way ANOVA, two-tailed, p=0.0993 F=2.536). Each circle represents the DT of an individual animal. The bar represents the mean DT of all animals of that group for last task. The error bars represent SEM.

(A4) ITI (Ordinary One-way ANOVA, two-tailed, p=0.3179 F=1.203), Each bar represents the mean ITI across animals of that group. The error bars represent the SEM

(A5) % Licked (Ordinary One-way ANOVA, two-tailed, p=0.6090 F=0.5064). (Figure on the next page). Each bar represents the mean % Licked across animals of that group. The error bars represent the SEM

From the flow coupled with odor discrimination task, it is observed that exposure to EE leads to a faster learning pace. When the learning efficiencies of the flow-only task, odor-only task and flow coupled with odor task are compared (Figure 15 Two-way ANOVA, p<0.0001 F=271.1, Tukey's Test), it is observed that the learning pace of flow-only task, which was performed first, is slowest. Compared to flow-only task, both odor-only and flow coupled with odor task have a faster learning pace. Finally, in the case of flow coupled with odor (performed last), pace of learning is more than odor-only and flow-only discrimination task.

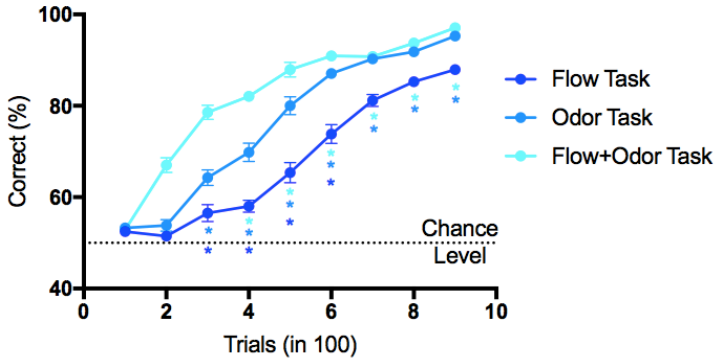

*Figure 15. Probable multisensory enhancement due to the presence of both mechanical and odorant stimuli. Learning efficiencies shown for enriched GAD2GluA2$^{\Delta ht}$ mice in case of odor-only, flow-only and flow coupled with odor discrimination task curve (Two-way ANOVA, p<0.0001 F=271.1, Tukey's Test, * p<0.05 for flow+odor task vs flow task, * p<0.05 for flow+odor task vs odor task, * p<0.05 flow task vs odor task). Compared to flow-only and odor-only task, the learning pace of flow coupled with odor task is faster. Each circle in the learning curve represents mean accuracy of 100 trials across all animals of that group. The error bars represent the SEM.*

3. 5. Environmental enrichment improves odor learning but not odor memory

To investigate the effect of EE on odor memory of GAD2GluA2$^{\Delta ht}$ mice, memory tasks were performed for the odor task and the flow coupled with odor task. It was performed 28 days after the half-reward tasks (see methods). As observed in Figure 16A1 (Unpaired t-test, two-tailed, p=0.6388 F=3.035), for the memory trials of odor task, there is no significant difference between the Enriched GAD2GluA2$^{\Delta ht}$ mice (~62%) and the Non-enriched GAD2GluA2$^{\Delta ht}$ mice (~61%). When the memory trials for the flow coupled with odor task were analyzed, again, no statistically significant difference was observed between the two groups (71.42% vs 71.02%) (Figure 16A2 Unpaired t-test, two-tailed, p=0.8556 F=4.361). Thus, enrichment did not seem to cause an improvement in memory for the above two odor/flow discrimination tasks.

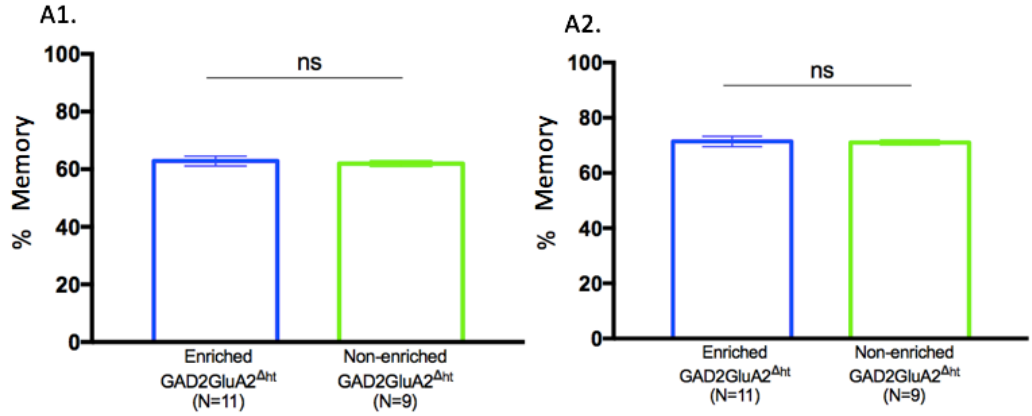

Figure 16. Memory tasks show that EE does not lead to improvement of odor memory

(*A1) Octanols (+/-) Binary Mixture (odor task) (Unpaired t-test, two-tailed, p=0.6388 F-value=3.035). The bar represents the mean % memory of all animals of that group. The error bars represent the SEM.*
(A2) Hexanal and Pentanone Binary Mixture, S+=0.4 S-=0.3 (flow coupled with odor task) (Unpaired t-test, two-tailed, p=0.8556 F-value=4.361). The bar represents the mean % memory of all animals of that group. The error bars represent the SEM.

Most studies have found an EE led improvement in case of spatial memory or age-related decline in memory (Kempermann, 2019). The effect of EE paradigm on olfactory memory remains unknown. In our case, memory for odor pair is being assessed 30 days after the behavioral task. Whether or not EE would lead to an improvement in an olfaction based memory task, remains to be investigated.

3. 6. Environmental enrichment leads to enhanced activation of inhibitory interneurons of Olfactory Bulb

Our results indicate that enrichment leads to rescue of learning deficits in GAD2GluA2$^{\Delta ht}$ mice. However, the neural mechanism governing this betterment remains elusive. A possible neural correlate could be an enhancement in the neural activity of the sensory regions which are involved in decision making and affected by EE. In order to address this, c-Fos, an early immediate gene marker was used as a readout of recent synaptic activity.

In order to check the c-Fos activity in the enriched and non-enriched GAD2GluA2$^{\Delta ht}$ mice, perfusion was performed within a time frame 90 minutes after a behavioral task was performed (adapted from Pfarr et al., 2018). The Hexanal and Pentanone binary mixture was coupled with 0.4 LPM and 0.3 LPM airflow rates. This discrimination task was the fourth and last behavior task performed by the mice. Thus, perfusion (and subsequent immunohistochemistry) was performed immediately after this discrimination task.

A1.

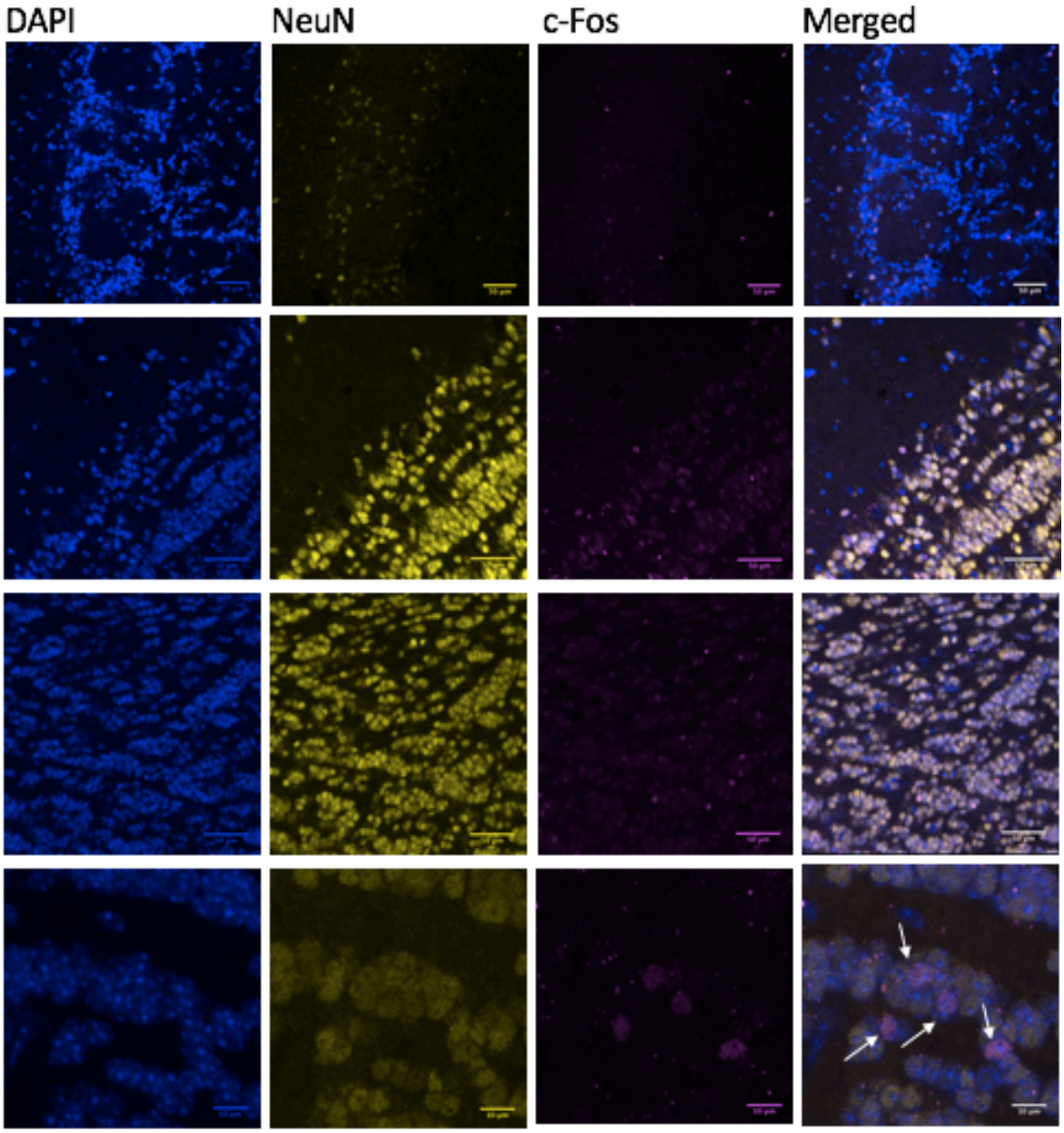
DAPI
NeuN
c-Fos
Merged

A2.

A3.

A4.

A5.

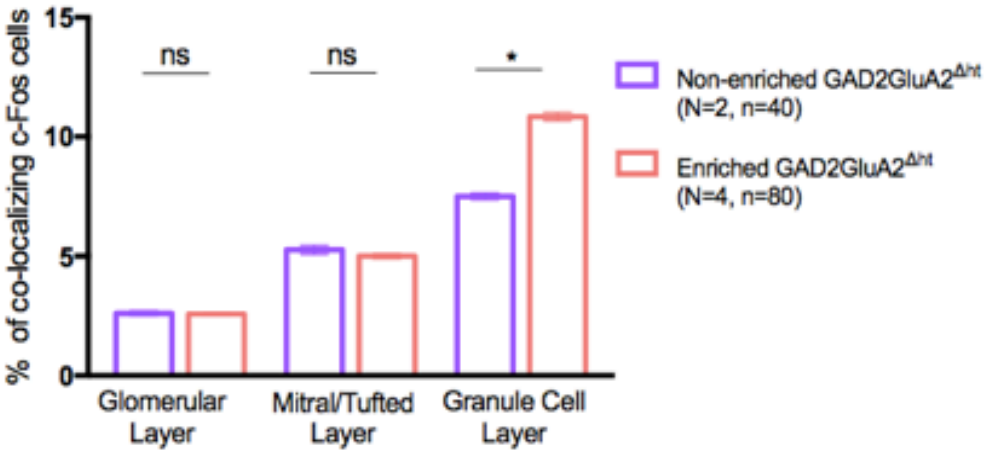
% of co-localizing c-Fos cells
15
10
5
0
ns
ns
*
Glomerular Layer
Mitral/Tufted Layer
Granule Cell Layer
Non-enriched GAD2GluA2Δ/ht (N=2, n=40)
Enriched GAD2GluA2Δ/ht (N=4, n=80)

Figure 17. EE dependent increase in GCL activation is observed using c-Fos staining and quantification.
(A1) Glomerular Layer representative image (40x),
(A2) Mitral Cell Layer representative image (40x),
(A3) Granule Cell Layer image (40x),
(A4) Representative Image of Granule cell layer c-Fos colocalization at 63x. White arrows marks the co-localized c-Fos+ cells,
(A5) % of co-localizing c-Fos cells in Non-enriched GAD2GluA2$^{\Delta ht}$ mice verses Enriched GAD2GluA2$^{\Delta ht}$ mice where N=no. of animals and n= field of views (FoVs) (GL: Unpaired t-test, two-tailed, p=0.8274 F=3.428, MCL: Unpaired t-test, two-tailed, p=0.2238 F=3.133, GCL: Unpaired t-test, two-tailed, p<0.0001 F=1.687). The bar represents the mean % co-localizing c-Fos cells across all animals of that group. The error bars represent the SEM. The FOVs or n are taken from 50 µm thick sections. *For each animal, approximately 5 sections per OB were chosen. For each OB section 12 FOVs were imaged.*

In the GL, the c-Fos activation observed was very less compared to MCL and GCL (Figure 17A1). Less c-Fos activation was also observed in MCL (Figure 17A2). The GCL, however, showed an increased c-Fos activation (Figure 17A3). DAPI, NeuN and c-Fos signal was also imaged at 63x to check for c-fos co-localization (Figure 17A4). The percentage of c-Fos positive cells co-localizing with DAPI positive cells were quantified. For the GL and MCL, the % of co-localizing c-Fos cells were comparable at around 2% (Unpaired t-test, two-tailed, p=0.8274 F=3.428) and 5% (Unpaired t-test, two-tailed, p=0.2238 F=3.133) respectively. However, in case of GCL, the % of co-localizing c-Fos cells were significantly higher in case of the enriched GAD2GluA2$^{\Delta ht}$ mice (10.84%) as compared to the non-enriched group (7.50%) (Unpaired t-test, two-tailed, p<0.0001 F=1.687) (Figure 17A5).

Thus, the enriched GAD2GluA2$^{\Delta ht}$ mice show an increased GCL activation as compared to the non-enriched group. This enrichment dependent enhancement in GCL activation might be leading to greater refinement of M/T responses and the observed improvement in airflow discrimination tasks. In this experiment, the impact

of both, behavioral training as well as EE on OB modulation was investigated. The effect of only EE or only training needs to explored.

3.7. Invariant neurogenesis between Enriched and Non-enriched GAD2GluA2$^{\Delta ht}$ mice

Numerous studies have connected increased hippocampal adult neurogenesis with the EE paradigm (Kempermann et al., 1997). Furthermore, unpublished data from our lab also suggests that exposure to EE leads to an increase in OB adult neurogenesis of wild type mice (Meenakshi Pardasani, LNCB). Thus, another possible hypothesis explaining the improvement in GAD2GluA2$^{\Delta ht}$ mice deficits could be an enrichment dependent increase in the number of adult born OB neurons. Enrichment could be leading to enhancement in adult neurogenesis, which would again lead to refinement of M/T responses and improved airflow discrimination abilities. In order to compare adult neurogenesis between the enriched and non-enriched GAD2GluA2$^{\Delta ht}$ mice, BrdU staining was performed. Three/four mice were chosen form each group and they were injected with BrdU 28 days before perfusion. When the number of BrdU+ cells were quantified for the both the groups, no significant difference was observed (Figure 18, Unpaired t-test, two-tailed, p=0.8703 F=4.358). For GAD2GluA2$^{\Delta ht}$ mice, exposure to an enriched environment was not leading to an increase in the number of BrdU+ cells.

A1.

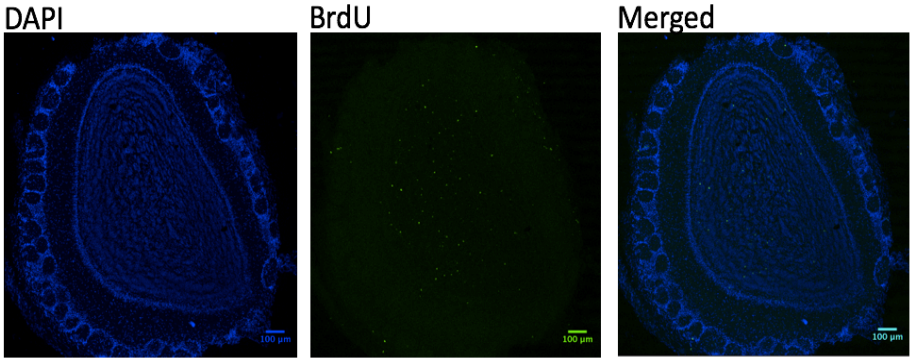

A2.

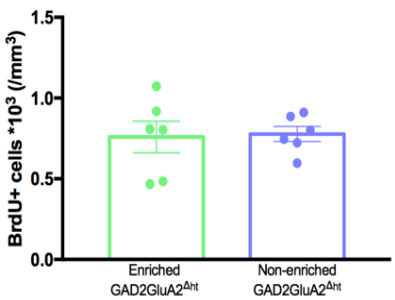

Figure 18. Number of BrdU+ cells is similar for the enriched and non-enriched group. (A1) Representative image of OB with BrdU staining (at 10x),
(A2) Number of BrdU+ cells in enriched GAD2GluA2$^{\Delta ht}$ mice (N= 3, n=6; where, N=number of animals, n=number of OBs) and non-enriched GAD2GluA2$^{\Delta ht}$ mice (N=3, n=6) (Unpaired t-test, two-tailed, p=0.8703 F-value=4.358). Each circle represents an OB section whereas the bar gives the mean of BrdU+ cells across all OB sections of N animals. The error bars denote the SEM.

Therefore, as observed from the above results, even though enrichment led to increased GCL activation, it showed no increase in the number of adult-born OB neurons.

4. Discussion

The environmental enrichment paradigm was used as a therapeutic intervention to investigate whether a rescue could be observed in the airflow rate discrimination deficits of GAD2GluA2$^{\Delta ht}$ mice. It was observed that following EE exposure, GAD2GluA2$^{\Delta ht}$ mice were able to discriminate between 0.35 LPM and 0.45 LPM with a better accuracy as compared to the non-enriched GAD2GluA2$^{\Delta ht}$ mice. The rescue in airflow discrimination was also reflected in the decreased discrimination time measurements. It was observed that the performance levels of enriched GAD2GluA2$^{\Delta ht}$ mice and enriched wild-type mice were very similar. A similar trend was observed when a second airflow pair discrimination task (0.1 vs 0.15 LPM) was carried out). These observations proved that enrichment led to the rescue of learning deficiency. It alludes to the fact that cognitive and sensory stimulation is indeed beneficial for the animal. It should be noted that even though GAD2GluA2$^{\Delta ht}$ mice had very high DT measurements in both the airflow discrimination tasks, variability was present in sample pattern as well as lick pattern DT (as observed in figure 11). DT values are distributed from 500ms to 1500ms. A point to also note here is that, stable DT measurements are calculated when the learning of the animals is above 80%. However, these transgenic mice show poor learning (not more than 60%, Figure 11B). Still, the variability in the observed DT measurements could be attributed to the fact that these transgenic mice are heterozygous. This implies that there would be varying levels of reduction in the GluA2 subunit of GAD2 expressing interneurons across these animals. It is possible that the mice which had faster DT measurements, had functional GluA2 subunit (lesser reduction). It is possible to investigate this hypothesis by performing receptor protein quantification (using Western Blotting) and comparing between mice with faster DTs and slower DTs.

In the odor discrimination task, the enriched GAD2GluA2$^{\Delta ht}$ mice had a faster learning pace as compared to non-enriched GAD2GluA2$^{\Delta ht}$ mice. However, this observation was not reflected in the discrimination time. It is possible that the two readouts, learning pace and discrimination time, reflect different paths of neuronal processing. Further, mice had to perform an airflow coupled with odor discrimination task, in which, enriched mice showed a faster learning pace compared to the non-

enriched group. This observation was seen in the case of learning efficiency, not the discrimination time. A question that is raised here is whether the presence of two stimuli (odor and flow) coupled together in a discrimination task is leading to multisensory enhancement and aiding the mice in performing better. One possibility could be that either both odor and flow contribute to the discrimination task, leading to multisensory enhancement, and faster learning. It is also possible that mice only pick up odor as a cue and discriminate between the stimuli. It is difficult to address this question using the experiments performed in this thesis, as odor-only task, flow-only task and flow coupled with odor discrimination task have been performed in the same group of mice (Figure 15). So, as mice perform sequential discrimination tasks, they get more familiar with the go/no-go procedure and betterment in conceptual learning may happen (Saar et al, 1998). Thus, each of these conditions can be tested with three separate sets of mice.

As mice perform successive odor discrimination tasks, there is also an improvement of the procedural learning since mice are now accustomed to the paradigm itself (Figure 15). This leads to faster learning in subsequent discrimination tasks. This kind of learning is called “rule learning” (Saar et al., 1998). It can be hypothesized that enrichment is facilitating a quicker grasp of rule learning. This could also explain the much faster learning pace of airflow rate coupled with odor task, as compared to odor-only or flow-only task (in case of enriched group). One of the neural mechanisms of odor rule learning is an enhanced synaptic connectivity between OB and Anterior Piriform Cortex (APC) (Barkai et al., 2014). The effect of enrichment on the connectivity of OB-APC pathway, and thus odor rule learning, is not known yet. Enrichment dependent changes in APC activity can also be investigated to address the question whether exposure to an enriched environment is affecting odor rule learning. An enhancement in the intrinsic excitability of neurons has also been explored as one of the neural mechanisms governing odor rule learning (Barkai, 2014). As a result of rule learning due to odor discrimination tasks, increase in neuronal excitability has been observed in the CA1 neurons of hippocampus (Zelcer et al., 2006). A separate study found out that due to exposure to an enriched environment, there was an enhancement of excitability in CA1 hippocampal neurons (Malik and Chattarji, 2011). Thus, from these studies, it can be hypothesized that enrichment is causing an increase in neuronal excitability in CA1 neurons of

hippocampus in case of GAD2GluA2$^{\Delta ht}$ mice, leading to an enhancement in odor rule learning. OB and hippocampus are bi-directionally connected. Projections from OB reach the hippocampus via synapses at PC and the Entorhinal Cortex (EC). The CA1 neurons of the hippocampus directly send projections to the GCL of OB (Martin et al., 2007). Thus, due to the strong interactions between the two regions, neuronal excitability in CA1 pyramidal neurons of hippocampus has an impact on odor rule learning. Activation of CA1 cells using immediate early gene markers can be performed, followed by electrophysiological recordings to dissect out the role of these neurons in enrichment dependent increase in learning pace.

While GAD2GluA2$^{\Delta ht}$ mice showed learning deficits in airflow discrimination tasks, no such deficits were observed during odor discrimination tasks. A recent study investigated activation patterns of OB due to airflow and odor stimulation using MRI. It was observed that airflow stimulation led to a much broader neural OB activation as compared to odor stimulation (Wu et al., 2017). In case of airflow information processing, it is possible that an optimized inhibition onto the M/T cells is required for the discrimination to occur. Due to knockdown of GluA2 from the GAD2 expressing interneuronal population, there is increased release of GABA onto the M/T cells. Thus, an increased inhibition in a broadly distributed manner in the GAD2GluA2$^{\Delta ht}$ mice could be leading to disruption of the optimized inhibition and causing airflow discrimination deficit. In order to investigate the above hypothesis, *in-vivo* electrophysiology can be performed in behaving GAD2GluA2$^{\Delta ht}$ mice, to quantify the inhibition onto the M/T cells which leads to the observed sensory deficit. In case of odor stimulation, since OB activation is localized, an increase in inhibition might lead to refinement on the M/T cells output, leading to faster learning. However, this is not observed when GAD2GluA2$^{\Delta ht}$ mice perform a complex odor discrimination task. It is possible that due to heterozygous nature of the GAD2GluA2$^{\Delta ht}$ mice, there is varying levels of inhibition onto M/T cells. So, odor discrimination is unaffected in GAD2GluA2$^{\Delta ht}$ mice. To address this, GluA2 can be knocked out specifically from GL and GCL followed by airflow and odor discrimination tasks.

Even though enrichment led to a faster learning pace in odor and flow coupled with odor task, no improvement was observed in odor memory tasks. Unpublished data

from the lab showed that enrichment did not lead to odor memory improvement in wild-type mice (Data from Meenakshi Pardasani). In a study published in 2005, forebrain specific GluA2 knock-out mice were created. These mice showed deficits in their olfactory memory. The memory impairment was rescued by expressing GluA2 in hippocampus and PC (Shimshek et al., 2005). The effect of GluA2 knockdown (in GAD2 expressing interneurons) on olfactory memory is yet to be investigated. To address this, wild-type animals (housed in standard home cage) can be utilized to perform the same sequence of experiments as followed in this thesis. This would shed light on whether GAD2GluA2$^{\Delta ht}$ mice have any odor memory deficits. According to a recent study, AON is involved in storage and retrieval of odor memory (Aqrabawi & Kim, 2020). Thus, to further probe the effect of enrichment on olfactory memory, enrichment dependent activation of AON neurons using c-Fos analysis can be investigated. NMDAR dependent plasticity has been shown to modulate olfactory learning and mediate the effect of daily enrichment (Mandairion et al 2006). At the level of synapse functioning, this can primarily affect Spike Timing Dependent Plasticity (STDP). STDP controls the excitability of neurons and the scaling of the inhibition of inhibitory neurons, thus, playing an important role in governing memory (Caporale & Dan, 2008).

Apart from an effect on synaptic plasticity, EE also leads to non-localized neuromodulatory changes. As EE dependent rescue in the airflow discrimination abilities of GAD2GluA2$^{\Delta ht}$ mice was observed due to enrichment, the next step was to probe for the possible underlying neural mechanisms. The EE paradigm affects the brain of an organism at multiple levels, from changes in neuronal structure to changes in levels of neurotrophic factors. Thus, due to the complex nature of environmental enrichment, it is highly difficult to pin-point towards a single mechanism of action. One of the many possible mechanisms could be enrichment leading to an enhanced activity of neurons involved in airflow information processing. Therefore, c-Fos activity was analyzed in different layers of OB. Being an early gene marker, c-Fos marks neurons which have been recently active (Bullitt, 1990. When the number of c-Fos positive cells which were co-localizing with DAPI positive cells was quantified across groups, it was observed that enriched GAD2GluA2$^{\Delta ht}$ mice showed a significant increase in the GCL activation. This implies, that while

performing a flow coupled with odor discrimination task, the GCs of enriched GAD2GluA2$^{\Delta ht}$ mice were more active. There was no difference in the c-Fos activity at the levels of GL and MCL. It is possible that enrichment is leading to increase in percentage of active GCs, leading to greater inhibition onto M/T cells and thus, refinement of the output. A more refined response from the M/T cell population could be leading to the improvements observed in airflow discrimination tasks. However, further experiments are required to be performed to corroborate this hypothesis. It is also possible that the increased c-Fos activity in GCL of enriched GAD2GluA2$^{\Delta ht}$ mice is because of increase in the number of the GCs itself. One of the mechanisms which leads to regular turnover and integration of GCs in the OB causing an increase in number of GCs is OB adult neurogenesis. In an unpublished study from the lab, enrichment dependent increase in adult neurogenesis was observed in the OB in case of wild-type mice (Data from Meenakshi Pardasani). In order to investigate the adult neurogenesis in the OB, BrdU immunostaining was performed for the enriched GAD2GluA2$^{\Delta ht}$ mice and the non-enriched GAD2GluA2$^{\Delta ht}$ mice. There was significant difference in the levels of adult neurogenesis between the two groups. Since the effect of GluA2 knockdown on OB adult neurogenesis has not been investigated yet, BrdU staining of wild-type mice should be performed to compare the number of adult-born OB neurons in GAD2GluA2$^{\Delta ht}$ group and wild-type group. (Figure 18).

The increased c-Fos activation in case of GCs of enriched GAD2GluA2$^{\Delta ht}$ mice could either be from the mature GCs or the newly born GCs. In order to address this, immunostaining for both c-Fos and BrdU cells can be performed. If the number of co-localizing c-Fos+ and BrdU+ cells are low, then more mature GCs are getting activated as a result of enrichment. More mature neurons are spatially located among superficial GCs (sGCs), and greater number of new-born GCs are integrated within deep GCs (dGCs) (Burton, 2017). This spatial separation can be used to dissect the major player (mature or new-born GCs) in the observed enrichment dependent increase in c-Fos activation.

Apart from these two hypotheses, which have been tested here, there could be more integrating mechanisms which could explain the rescue in airflow processing. A study has shown that exposure to an EE paradigm led to increase in the mRNA

expression as well as protein expression of GluA2 in the case of hippocampus (Naka et al., 2005). It is possible that, a similar increase in GluA2 expression is occurring in OB due to EE exposure. As the GAD2GluA2$^{\Delta ht}$ mice are heterozygous, GAD2 expressing interneurons would have varying levels of reduction in GluA2 subunit. GluA2 in those interneurons might increase, ultimately leading to improvement of the rescue of sensory deficit. In order to address this, western blotting needs to be performed to quantify the GluA2 expression in the OB, in case of enriched verses non-enriched GAD2GluA2$^{\Delta ht}$ mice. An important characterization (using Western Blotting) would also be quantifying the amount of GluA2 decrease observed in GAD2GluA2$^{\Delta ht}$ mice. This is an on-going experiment in our lab (Shruti Marathe, LNCB).

The expression of neurotrophic factors like Brain Derived Neurotrophic Factor (BDNF) and Vascular Endothelial Growth Factor (VEGF) also increases due to enrichment. (Clemenson et al., 2015). Both BDNF and VEGF also have a role to play in functioning of OB adult born neurons. VEGF is involved in the formation of dendrites (dendritogenesis) in the newborn interneurons (Licht et al., 2010). Administration of BDNF in brains of adult rats was shown to increase the number of adult born OB neurons (Zigova et al., 1998). Thus, in case of enriched GAD2GluA2$^{\Delta ht}$ mice, an increase in the expression of BDNF and VEGF might be occurring, leading to refinement of the output responses, and thus a rescue in the observed sensory deficit.

The specific contribution of olfactory enrichment in the observed EE-dependent airflow discrimination improvements in GAD2GluA2$^{\Delta ht}$ mice can also be investigated. Thus, an experiment needs to be conducted wherein GAD2GluA2$^{\Delta ht}$ mice are exposed to an enriched environment but without olfactory enrichment. If there is a reduction in the accuracy of mice performing airflow discrimination tasks, it would imply that the olfactory enrichment indeed particularly has an impact on the observed improvements.

To gain further insight on the role of OB circuitry in airflow processing, specific knockouts can be generated using viral injections. GluA2 can be specifically knocked out from the GCL (and/or GL). The mice can then be made to perform airflow

discrimination tasks. If a deficit is observed, the mice can be exposed to an enriched environment to investigate whether any betterment can be seen. The above experiment is going on in our lab (being performed by Shruti Marathe, LNCB).

Thus, as a part of this thesis, the dynamics between nature and nurture were explored. It was found that environmental enrichment does have a positive effect on airflow information processing in mice. Enrichment led to a rescue in an airflow learning deficit in GAD2GluA2$^{\Delta ht}$ mice. This study opens up avenues for further investigation of the role of OB circuitry in airflow information processing and the effect that environmental enrichment would have on this neural circuitry.

5. References

Abraham, N. M., Egger, V., Shimshek, D. R., Renden, R., Fukunaga, I., Sprengel, R., Seeburg, P. H., Klugmann, M., Margrie, T. W., Schaefer, A. T., & Kuner, T. (2010). Synaptic Inhibition in the Olfactory Bulb Accelerates Odor Discrimination in Mice. *Neuron*. https://doi.org/10.1016/j.neuron.2010.01.009

Abraham, N. M., Spors, H., Carleton, A., Margrie, T. W., Kuner, T., & Schaefer, A. T. (2004). Maintaining accuracy at the expense of speed: Stimulus similarity defines odor discrimination time in mice. *Neuron*. https://doi.org/10.1016/j.neuron.2004.11.017

Alwis, D. S., & Rajan, R. (2014). Environmental enrichment and the sensory brain: The role of enrichment in remediating brain injury. In *Frontiers in Systems Neuroscience*. https://doi.org/10.3389/fnsys.2014.00156

Aqrabawi, A. J., & Kim, J. C. (2020). Olfactory memory representations are stored in the anterior olfactory nucleus. *Nature Communications*. https://doi.org/10.1038/s41467-020-15032-2

Arabzadeh, E., Panzeri, S., & Diamond, M. E. (2004). Whisker vibration information carried by rat barrel cortex neurons. *Journal of Neuroscience*. https://doi.org/10.1523/JNEUROSCI.1389-04.2004

Arabzadeh, E., Petersen, R. S., & Diamond, M. E. (2003). Encoding of whisker vibration by rat barrel cortex neurons: Implications for texture discrimination. *Journal of Neuroscience*. https://doi.org/10.1523/jneurosci.23-27-09146.2003

Barkai, E. (2014). Neural mechanisms of odor rule learning. In *Progress in Brain Research*. https://doi.org/10.1016/B978-0-444-63350-7.00010-3

Barone, I., Novelli, E., & Strettoi, E. (2014). Long-term preservation of cone photoreceptors and visual acuity in rd10 mutant mice exposed to continuous environmental enrichment. *Molecular Vision*.

Bax, C., Sironi, S., & Capelli, L. (2020). How Can Odors Be Measured? An Overview of Methods and Their Applications. *Atmosphere*. https://doi.org/10.3390/atmos11010092

Bennett, E. L., Rosenzweig, M. R., & Diamond, M. C. (1969). Rat brain: Effects of environmental enrichment on wet and dry weights. *Science*. https://doi.org/10.1126/science.163.3869.825

Bonzano, S., Bovetti, S., Fasolo, A., Peretto, P., & De Marchis, S. (2014). Odour enrichment increases adult-born dopaminergic neurons in the mouse olfactory bulb. *European Journal of Neuroscience*. https://doi.org/10.1111/ejn.12724

Boubenec, Y., Shulz, D. E., & Debrégeas, G. (2012). Whisker encoding of mechanical events during active tactile exploration. *Frontiers in Behavioral Neuroscience*.

Bouton, M. E., & Sunsay, C. (2001). Contextual control of appetitive conditioning: Influence of a contextual stimulus generated by a partial reinforcement procedure. *Quarterly Journal of Experimental Psychology Section B: Comparative and Physiological Psychology*. https://doi.org/10.1080/02724990042000083

Brown, R. E., & Milner, P. M. (2003). The legacy of Donald O. Hebb: More than the Hebb Synapse. In *Nature Reviews Neuroscience*. https://doi.org/10.1038/nrn1257

Bullitt, E. (1990). Expression of C-fos-like protein as a marker for neuronal activity following noxious stimulation in the rat. *Journal of Comparative Neurology*. https://doi.org/10.1002/cne.902960402

Bumbalo, R., Lieber, M., Schroeder, L., Polat, Y., Breer, H., & Fleischer, J. (2017). Grueneberg Glomeruli in the Olfactory Bulb are Activated by Odorants and Cool Temperature. *Cellular and Molecular Neurobiology*. https://doi.org/10.1007/s10571-016-0408-6

Burton, S. D. (2017). Inhibitory circuits of the mammalian main olfactory bulb. In *Journal of Neurophysiology*. https://doi.org/10.1152/jn.00109.2017

Caporale, N., & Dan, Y. (2008). Spike Timing–Dependent Plasticity: A Hebbian Learning Rule. *Annual Review of Neuroscience*. https://doi.org/10.1146/annurev.neuro.31.060407.125639

Clemenson, G. D., Deng, W., & Gage, F. H. (2015). Environmental enrichment and neurogenesis: From mice to humans. In *Current Opinion in Behavioral Sciences*. https://doi.org/10.1016/j.cobeha.2015.02.005

Engineer, N. D., Percaccio, C. R., Pandya, P. K., Moucha, R., Rathbun, D. L., & Kilgard, M. P. (2004). Environmental enrichment improves response strength, threshold, selectivity, and latency of auditory cortex neurons. *Journal of Neurophysiology*. https://doi.org/10.1152/jn.00059.2004

Getchell, T. V., Margolis, F. L., & Getchell, M. L. (1984). Perireceptor and receptor events in vertebrate olfaction. In *Progress in Neurobiology*. https://doi.org/10.1016/0301-0082(84)90008-X

Gratzner, H. G. (1982). Monoclonal antibody to 5-bromo- and 5-iododeoxyuridine: A new reagent for detection of DNA replication. *Science*. https://doi.org/10.1126/science.7123245

Grosmaitre, X., Santarelli, L. C., Tan, J., Luo, M., & Ma, M. (2007). Dual functions of mammalian olfactory sensory neurons as odor detectors and mechanical sensors. *Nature Neuroscience*. https://doi.org/10.1038/nn1856

Imai, T., & Sakano, H. (2008). Odorant receptor-mediated signaling in the mouse. In *Current Opinion in Neurobiology*. https://doi.org/10.1016/j.conb.2008.07.009

Isaacson, J. S., & Strowbridge, B. W. (1998). Olfactory reciprocal synapses: Dendritic signaling in the CNS. *Neuron*. https://doi.org/10.1016/S0896-6273(00)81013-2

Jung, C. K. E., & Herms, J. (2014). Structural dynamics of dendritic spines are influenced by an environmental enrichment: An in vivo imaging study. *Cerebral Cortex*. https://doi.org/10.1093/cercor/bhs317

Kempermann, G. (2019). Environmental enrichment, new neurons and the neurobiology of individuality. In *Nature Reviews Neuroscience*. https://doi.org/10.1038/s41583-019-0120-x

Kempermann, G., Kuhn, H. G., & Gage, F. H. (1997). More hippocampal neurons in adult mice living in an enriched environment. *Nature*. https://doi.org/10.1038/386493a0

Koh, S., Magid, R., Chung, H., Stine, C. D., & Wilson, D. N. (2007). Depressive behavior and selective downregulation of serotonin receptor expression after early-life seizures: Reversal by environmental enrichment. *Epilepsy and Behavior*. https://doi.org/10.1016/j.yebeh.2006.11.008

Kwak, S., & Kawahara, Y. (2005). Deficient RNA editing of GluR2 and neuronal death in amyotropic lateral sclerosis. In *Journal of Molecular Medicine*. https://doi.org/10.1007/s00109-004-0599-z

Lagier, S., Carleton, A., & Lledo, P. M. (2004). Interplay between Local GABAergic Interneurons and Relay Neurons Generates γ Oscillations in the Rat Olfactory Bulb. *Journal of Neuroscience*. https://doi.org/10.1523/JNEUROSCI.5570-03.2004

Lemessurier, A. M., Laboy-Juiárez, K. J., McCiain, K., Chen, S., Nguyen, T., & Feldman, D. E. (2019). Enrichment drives emergence of functional columns and improves sensory coding in the whisker map in L2/3 of mouse S1. *ELife*. https://doi.org/10.7554/eLife.46321

Licht, T., Eavri, R., Goshen, I., Shlomai, Y., Mizrahi, A., & Keshet, E. (2010). VEGF is required for dendritogenesis of newly born olfactory bulb interneurons. *Development*. https://doi.org/10.1242/dev.039636

Lledo, P. M., Alonso, M., & Grubb, M. S. (2006). Adult neurogenesis and functional plasticity in neuronal circuits. In *Nature Reviews Neuroscience*. https://doi.org/10.1038/nrn1867

Ma, M. (2009). Multiple olfactory subsystems convey various sensory signals. In *The Neurobiology of Olfaction*. https://doi.org/10.1201/9781420071993-c9

Malik, R., & Chattarji, S. (2012). Enhanced intrinsic excitability and EPSP-spike coupling accompany enriched environment-induced facilitation of LTP in hippocampal CA1 pyramidal neurons. *Journal of Neurophysiology*. https://doi.org/10.1152/jn.01009.2011

Mandairon, N., Stack, C., Kiselycznyk, C., & Linster, C. (2006). Broad activation of the olfactory bulb produces long-lasting changes in odor perception. *Proceedings of the National Academy of Sciences of the United States of America*. https://doi.org/10.1073/pnas.0602750103

Margrie, T. W., Sakmann, B., & Urban, N. N. (2001). Action potential propagation in mitral cell lateral dendrites is decremental and controls recurrent and lateral inhibition in the mammalian olfactory bulb. *Proceedings of the National Academy of Sciences of the United States of America*. https://doi.org/10.1073/pnas.98.1.319

Martin, C., Beshel, J., & Kay, L. M. (2007). An olfacto-hippocampal network is dynamically involved in odor-discrimination learning. *Journal of Neurophysiology*. https://doi.org/10.1152/jn.00524.2007

Mori, K., & Sakano, H. (2011). How Is the Olfactory Map Formed and Interpreted in the Mammalian Brain? *Annual Review of Neuroscience*. https://doi.org/10.1146/annurev-neuro-112210-112917

Nagayama, S., Homma, R., & Imamura, F. (2014). Neuronal organization of olfactory bulb circuits. In *Frontiers in Neural Circuits*. https://doi.org/10.3389/fncir.2014.00098

Naka, F., Narita, N., Okado, N., & Narita, M. (2005). Modification of AMPA receptor properties following environmental enrichment. *Brain and Development*. https://doi.org/10.1016/j.braindev.2004.07.006

Parrish-Aungst, S., Shipley, M. T., Erdelyi, F., Szabo, G., & Puche, A. C. (2007). Quantitative analysis of neuronal diversity in the mouse olfactory bulb. *Journal of Comparative Neurology*. https://doi.org/10.1002/cne.21205

Pfarr, S., Schaaf, L., Reinert, J. K., Paul, E., Herrmannsdörfer, F., Roßmanith, M., Kuner, T., Hansson, A. C., Spanagel, R., Körber, C., & Sommer, W. H. (2018). Choice for drug or natural reward engages largely overlapping neuronal ensembles in the infralimbic prefrontal cortex. *Journal of Neuroscience*. https://doi.org/10.1523/JNEUROSCI.0026-18.2018

Pham, T. M., Ickes, B., Albeck, D., Söderström, S., Granholm, A. C., & Mohammed, A. H. (1999). Changes in brain nerve growth factor levels and nerve growth factor receptors in rats exposed to environmental enrichment for one year. *Neuroscience*. https://doi.org/10.1016/S0306-4522(99)00316-4

Por, S. B., Bennett, E. L., & Bondy, S. C. (1982). Environmental enrichment and neurotransmitter receptors. *Behavioral and Neural Biology*. https://doi.org/10.1016/S0163-1047(82)91514-X

Rall, W., & Shepherd, G. M. (1968). Theoretical reconstruction of field potentials and dendrodendritic synaptic interactions in olfactory bulb. *Journal of Neurophysiology*. https://doi.org/10.1152/jn.1968.31.6.884

Rochefort, C., Gheusi, G., Vincent, J. D., & Lledo, P. M. (2002). Enriched Odor Exposure Increases the Number of Newborn Neurons in the Adult Olfactory Bulb and Improves Odor Memory. *Journal of Neuroscience*. https://doi.org/10.1523/jneurosci.22-07-02679.2002

Rosenzweig, M. R., & Bennett, E. L. (1996). Psychobiology of plasticity: Effects of training and experience on brain and behavior. *Behavioural Brain Research*. https://doi.org/10.1016/0166-4328(95)00216-2

Saar, D., Grossman, Y., & Barkai, E. (1999). Reduced synaptic facilitation between pyramidal neurons in the piriform cortex after odor learning. *Journal of Neuroscience*. https://doi.org/10.1523/jneurosci.19-19-08616.1999

Shepherd, G. M., Chen, W. R., & Greer, C. A. (2004). Olfactory Bulb. In *The Synaptic Organization of the Brain*. https://doi.org/10.1093/acprof:oso/9780195159561.003.0005

Shepherd, G. M., Chen, W. R., Willhite, D., Migliore, M., & Greer, C. A. (2007). The olfactory granule cell: From classical enigma to central role in olfactory processing. In *Brain Research Reviews*. https://doi.org/10.1016/j.brainresrev.2007.03.005

Shimshek, D. R., Bus, T., Kim, J., Mihaljevic, A., Mack, V., Seeburg, P. H., Sprengel, R., & Schaefer, A. T. (2005). Enhanced odor discrimination and impaired olfactory memory by spatially controlled switch of AMPA receptors. *PLoS Biology*. https://doi.org/10.1371/journal.pbio.0030354

Sobolevsky, A. I., Rosconi, M. P., & Gouaux, E. (2009). X-ray structure, symmetry and mechanism of an AMPA-subtype glutamate receptor. *Nature*. https://doi.org/10.1038/nature08624

UEKI, S., & DOMINO, E. F. (1961). Some evidence for a mechanical receptor in olfactory function. *Journal of Neurophysiology*. https://doi.org/10.1152/jn.1961.24.1.12

Wright, A., & Vissel, B. (2012). The essential role of AMPA receptor GluA2 subunit RNA editing in the normal and diseased brain. In *Frontiers in Molecular Neuroscience*. https://doi.org/10.3389/fnmol.2012.00034

Woolsey, T., & Van der Loos, H. (1970). The structural organization of layer IV in the somatosensory region (S I) of mouse cerebral cortex. *Brain Research*, *17*(2), 205-242. doi: 10.1016/0006-8993(70)90079-x

Wu, H., Jin, Y., Buddhala, C., Osterhaus, G., Cohen, E., Jin, H., Wei, J., Davis, K., Obata, K., & Wu, J. Y. (2007). Role of glutamate decarboxylase (GAD) isoform, GAD65, in GABA synthesis and transport into synaptic vesicles-Evidence from

GAD65-knockout mice studies. *Brain Research*. https://doi.org/10.1016/j.brainres.2007.04.008'

Wu, R., Liu, Y., Wang, L., Li, B., & Xu, F. (2017). Activity patterns elicited by airflow in the olfactory bulb and their possible functions. *Journal of Neuroscience*. https://doi.org/10.1523/JNEUROSCI.2210-17.2017

Yamaguchi, M., & Mori, K. (2005). Critical period for sensory experience-dependent survival of newly generated granule cells in the adult mouse olfactory bulb. *Proceedings of the National Academy of Sciences of the United States of America*. https://doi.org/10.1073/pnas.0406082102

Yu, Y. S. W., Graff, M. M., Bresee, C. S., Man, Y. B., & Hartmann, M. J. Z. (2016). Whiskers aid anemotaxis in rats. *Science Advances*. https://doi.org/10.1126/sciadv.1600716

Yu, Y. S. W., Graff, M. M., & Hartmann, M. J. Z. (2016). Mechanical responses of rat vibrissae to airflow. *Journal of Experimental Biology*. https://doi.org/10.1242/jeb.126896

Zelcer, I., Cohen, H., Richter-Levin, G., Lebiosn, T., Grossberger, T., & Barkai, E. (2006). A cellular correlate of learning-induced metaplasticity in the hippocampus. *Cerebral Cortex*. https://doi.org/10.1093/cercor/bhi125

Zhao, K., & Frye, R. E. (2015). Nasal Patency and the Aerodynamics of Nasal Airflow in Relation to Olfactory Function. In *Handbook of Olfaction and Gustation: Third Edition*. https://doi.org/10.1002/9781118971758.ch16

Zigova, T., Pencea, V., Wiegand, S. J., & Luskin, M. B. (1998). Intraventricular administration of BDNF increases the number of newly generated neurons in the adult olfactory bulb. *Molecular and Cellular Neurosciences*. https://doi.org/10.1006/mcne.1998.0684

6. Supplementary Information

Supplementary Figure 1.

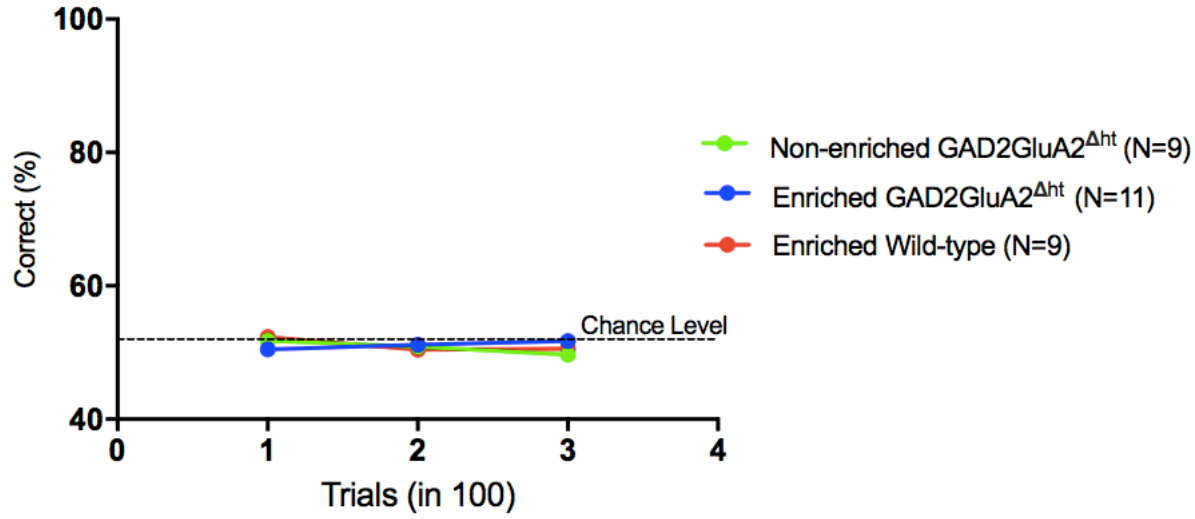

Figure S1. Control Task performed for the three groups, where both S+ and S- is 0.6 LPM. The performance of all three groups is chance-level. (Two-way ANOVA, p=0.7518 F=0.2864, Tukey's Test). Each circle in the learning curve represents mean accuracy of 100 trials across all animals of that group. The whiskers represent the SEM.

Supplementary Figure 2.

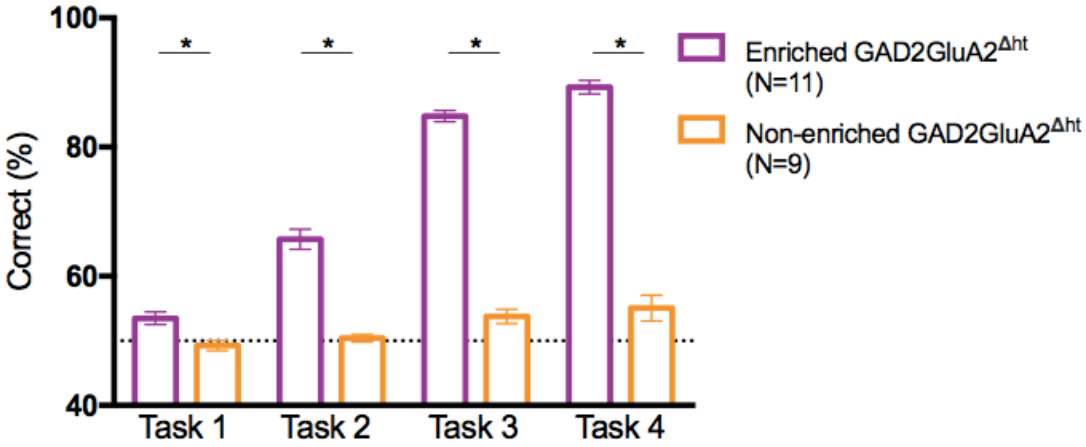

Figure S2. Learning efficiency for 0.35 vs 0.45 LPM airflow discrimination as the tasks progress. Enriched GAD2GluA2$^{\Delta ht}$ mice show increase in learning accuracy (in %) as tasks progress (from task1 to task 4, 300 trials per task). Comparatively, non-enriched GAD2GluA2$^{\Delta ht}$ mice show significantly poor learning (chance-level) (Task 1: Unpaired t-test, two-tailed, p=0.0043 F=1.851, Task 2: Unpaired t-test, two-tailed,

p<0.0001 F=8.719, Task 3: Unpaired t-test, two-tailed, p<0.0001 F=1.367, Task 4: Unpaired t-test, two-tailed, p<0.0001 F=3.044). Each bar represents the mean correct % across all animals of that particular group. The error bars denote the SEM.

Supplementary Figure 3.

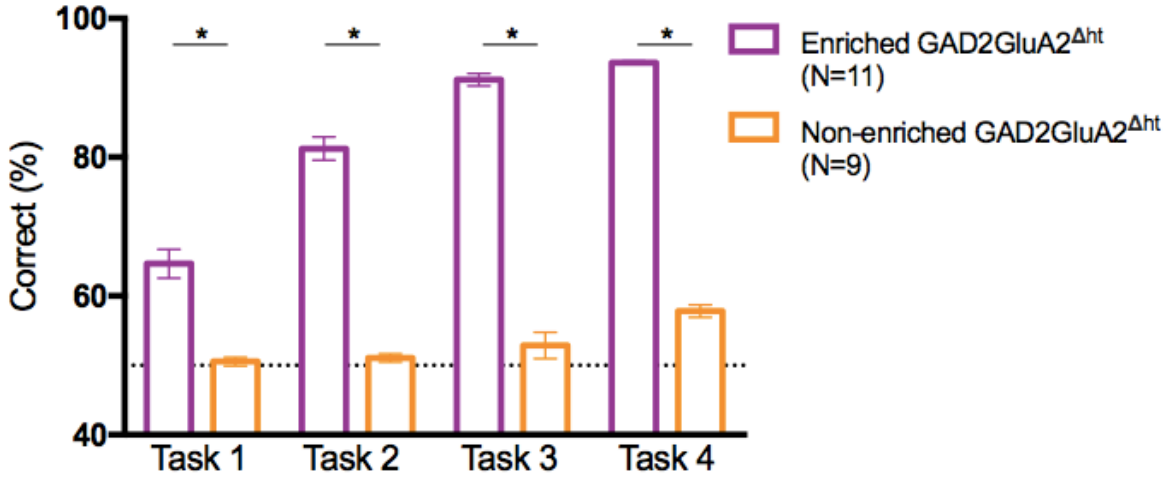

Figure S3. Learning efficiency for 0.10 vs 0.15 LPM airflow discrimination as the tasks progress. Enriched GAD2GluA2$^{\Delta ht}$ mice show increase in learning accuracy (in %) as tasks progress (from task1 to task 4, 300 trials per task). Comparatively, non-enriched GAD2GluA2$^{\Delta ht}$ mice show significantly poor learning (chance-level) (Task 1: Unpaired t-test, two-tailed, p<0.0001 F=13.37, Task 2: Unpaired t-test, two-tailed, p<0.0001 F=10.37, Task 3: Unpaired t-test, two-tailed, p<0.0001 F=3.704, Task 4: Unpaired t-test, two-tailed, p<0.0001 F=10.35). Each bar represents the mean correct % across all animals of that particular group. The error bars denote the SEM.